IMMUNOLOGY

JAK3 inhibitor suppresses multipotent ILC2s and attenuates steroid-resistant asthma

Jihyun Kim[1,2], Jongho Ham[1,2,3], Hye Ryun Kang[2,4], Yong-Soo Bae[3,5], TaeSoo Kim[6], Hye Young Kim[1,2,3]*

Steroids are the standard treatment for allergic airway inflammation in asthma, but steroid-refractory asthma poses a challenge. Group 2 innate lymphoid cells (ILC2s), such as T helper 2 (T_H2) cells, produce key asthma-related type 2 cytokines. Recent insights from mouse and human studies indicate a potential connection between ILC2s and steroid-resistant asthma. Here, we highlight that lung ILC2s, rather than T_H2 cells, can develop steroid resistance, allowing them to persist and maintain their disease-driving activity even during steroid treatment. The emergence of multipotent IL-5$^+$IL-13$^+$IL-17A$^+$ ILC2s is associated with steroid-resistant ILC2s. The Janus kinase 3 (JAK3)/signal transducer and activator of transcription (STAT) 3, 5, and 6 pathways contribute to the acquisition of steroid-resistant ILC2s. The JAK3 inhibitor reduces ILC2 survival, proliferation, and cytokine production in vitro and ameliorates ILC2-driven *Alternaria*-induced asthma. Furthermore, combining a JAK3 inhibitor with steroids results in the inhibition of steroid-resistant asthma. These findings suggest a potential therapeutic approach for addressing this challenging condition in chronic asthma.

INTRODUCTION

Asthma is a chronic respiratory disease characterized by airflow limitation and mucus hyperproduction, leading to persistent and spasmodic symptoms such as dyspnea, coughing, and wheezing (*1*). While the term "asthma" encompasses multiple phenotypes, the most common is allergic asthma (*2*). Type 2 inflammation mediates allergic asthma, involving the production of cytokines, such as interleukin-4 (IL-4), IL-5, IL-9, and IL-13. These cytokines are produced by T helper 2 (T_H2) cells and group 2 innate lymphoid cells (ILC2s), playing critical roles in asthma symptoms (*3*). Specifically, they induce eosinophil recruitment, goblet cell metaplasia, bronchial hyperreactivity, immunoglobulin E production, and mast cell activation. The primary treatment for persistent asthma is inhaled corticosteroids (*4*), which regulate the activities of various inflammatory cells to control asthma symptoms, improve lung function, and prevent exacerbation of the disease (*5*). However, 10% of asthmatics do not respond to steroids (*6*), and this steroid-resistant asthma holds considerable importance as it is associated with substantial asthma-related mortality and accounts for almost 50% of the annual asthma-associated health care costs (*7*). Therefore, an urgent and unmet clinical need in the field is a therapeutic approach that effectively treats steroid-resistant asthma. One approach to developing such treatments may be to improve our understanding of the immunological mechanisms that mediate steroid resistance in asthma patients.

ILC2s play a crucial role in the development of allergic asthma as they are activated downstream of airway epithelial cells. When faced with various triggers like external allergens, viral and bacterial elements, cigarette smoke, and inflammatory substances, the epithelial cells respond by generating alarmins such as IL-33, IL-25, and thymic stromal lymphopoietin (TSLP). These cytokines, in turn, stimulate ILC2s to produce abundant IL-5 and IL-13, as well as IL-4, IL-9, and amphiregulin (*8*). This ability to secrete large amounts of type 2 cytokines makes ILC2s a major focus of research on type 2 immune disorders, including chronic rhinosinusitis with nasal polyps, atopic dermatitis, and T2 asthma. The role of ILC2s in steroid-resistant asthma remains uncertain, with conflicting evidence reported in several studies. While some studies suggest that ILC2s may contribute to steroid resistance, others have found that ILC2s can be sensitive to steroids. For instance, one study found that patients with steroid-resistant asthma have more ILC2s in their sputum than control asthma patients (*9*), and another study in mice showed that the induction of steroid-resistant asthma was associated with the accumulation of steroid-resistant ILC2s in the lung (*10*). In contrast, other studies have reported that ILC2s can be reduced by steroid treatment in patients with nasal polyps or well-controlled asthma (*9*, *11*, *12*). Therefore, further research is needed to elucidate the complex role of ILC2s in steroid-resistant asthma.

T cells require activation of the "T cell" receptor to trigger the activation of several factors, such as nuclear factor kappa-light-chain-enhancer of activated B cells (NF-κB), activator protein 1, and nuclear factor of activated T cells, which stimulate T cell activity. Conversely, ILCs do not have antigen-specific receptors and instead rely on their cytokine receptors to respond to environmental signals. Cytokines, such as IL-2, IL-4, IL-7, IL-9, and TSLP, stimulate ILCs by activating Janus kinase 1 (JAK1), JAK3, and signal transducer and activator of transcription (STAT) molecules. These signaling pathways are vital for ILC biology, including their development, early effector functions, and plasticity (*13*–*15*). Consequently, this pathway presents a promising target for therapeutic intervention in ILC-mediated diseases. Pharmacological inhibitors

[1]Laboratory of Mucosal Immunology, Department of Biomedical Sciences, Seoul National University College of Medicine, Seoul, South Korea. [2]Institute of Allergy and Clinical Immunology, Seoul National University Medical Research Center, Seoul, South Korea. [3]Department of Biological Sciences, SRC Center for Immune Research on Non-lymphoid Organs, Sungkyunkwan University, Suwon, South Korea. [4]Department of Internal Medicine, Seoul National University Hospital, Seoul, South Korea. [5]Department of Biological Sciences, Sungkyunkwan University, Suwon, South Korea. [6]Department of Life Science, Multitasking Macrophage Research Center, Ewha Womans University, Seoul, South Korea.
*Corresponding author. Email: hykim11@snu.ac.kr

of JAK activity have been successful in treating various immune-mediated diseases (*16*).

Here, we demonstrated that ILC2s contribute to steroid-resistant asthma in murine models and can be converted into steroid-resistant ILC2s through exposure to multiple ILC-stimulating cytokines. Specifically, we found that the combination of IL-33 and TSLP or IL-33 and IL-2/IL-7 induced the emergence of multipotent ILC2s that secrete both IL-17A and type 2 cytokines, rendering them resistant to steroids. Our studies further revealed that the JAK3-mediated signaling pathway and phosphorylation of multiple STATs drove the formation of these multipotent ILC2s. Notably, we observed that blocking the JAK3 signaling pathway effectively inhibited the formation of the multipotent ILC2s in vitro and ameliorated ILC2-driven *Alternaria*-induced asthma. Combining JAK3 inhibitors with steroids to suppress asthmogenic T_H2 cells resulted in a marked inhibition of steroid-resistant asthma, accompanied by the disappearance of the multipotent ILC2s in vivo. These results highlight the potential of ILC2s as a therapeutic target for steroid-resistant asthma and the JAK3 inhibitor as a promising treatment option.

RESULTS

IL-33–induced ILC2s are responsible for steroid-resistant eosinophilia in a mouse model of asthma

A classical model of allergic asthma involves sensitizing wild-type mice with intraperitoneal injections of ovalbumin (OVA) followed by intratracheal challenge with OVA a week later (*17*). This model is driven largely by T_H2 cells and is highly sensitive to steroids (*18*). However, in the OVA/IL-33 mouse model of steroid-resistant asthma, which was reported by Kabata *et al.* (*10*), OVA-sensitized mice are challenged intratracheally with OVA plus IL-33 (Fig. 1A). During the challenge periods, OVA-alone and OVA/IL-33 asthma model mice were injected intraperitoneally with dexamethasone (Dex) (Fig. 1A). In the OVA-alone model, Dex significantly reduced airway hyperresponsiveness (AHR) (Fig. 1B) and eosinophilia a day after the last challenge/treatment (Fig. 1, D and E). However, in the OVA/IL-33 model, Dex failed to reduce AHR (Fig. 1C), airway eosinophil numbers (Fig. 1D), and inflammatory cell infiltration into the airways (Fig. 1E), indicating significantly reduced corticosteroid sensitivity. Notably, a key difference between the two models was that Dex suppressed the eosinophilia in the OVA-alone model but not in the OVA/IL-33 model. Steroid treatment, however, suppressed airway neutrophil, alveolar macrophage, and dendritic cell numbers equally well in both models (fig. S1, A to E).

Because IL-33 is a potent stimulator of ILC2s (*19*), we aimed to investigate whether ILC2s are responsible for the steroid-resistant eosinophilia observed in OVA/IL-33 mice. We analyzed the secretion of type 2 cytokines by ILC2s and T cells in the lungs of both models. In the OVA-alone model, $CD4^+$ T cells, not ILC2s, were found to secrete increased amounts of IL-5 and IL-13 (Fig. 1F). However, in the OVA/IL-33 model, both $CD4^+$ T cells and ILC2s secreted elevated levels of these cytokines (Fig. 1F). When treated with Dex, the OVA-alone mice showed a decrease in the production of IL-5 and IL-13 by $CD4^+$ T cells, while ILC2s continued to secrete these cytokines. Also, Dex suppressed $CD4^+$ T cell production of cytokines in the OVA/IL-33 model but failed to downregulate the secretion of these cytokines by ILC2s (Fig. 1, F to J). These findings suggest that ILC2s in the lungs could be responsible for the corticosteroid resistance observed in airway inflammation with eosinophilia.

Combined IL-33 and TSLP induces steroid-resistant asthma by generating steroid-resistant ILC2s

Previous studies have shown that blocking TSLP in murine asthma models or human asthmatics can restore steroid sensitivity in asthma (*10*, *20*). It suggests that elicitation of this alarmin during asthma pathogenesis may promote steroid resistance. Given this, and the fact that TSLP is an activator of ILC2s along with IL-33 (*21*), we investigated whether intratracheal injections of IL-33 plus TSLP would generate an ILC2-dependent steroid-resistant asthma model (Fig. 2A). Our findings indicate that IL-33/TSLP treatment induced AHR, and Dex treatment failed to reverse this (Fig. 2B). The inability of Dex to suppress eosinophilia was also observed; while IL-33/TSLP treatment induced the infiltration of eosinophils, neutrophils, and lymphocytes into the bronchoalveolar lavage fluid (BALF) and lungs, Dex only suppressed the increased neutrophil and lymphocyte numbers (Fig. 2, C and D, and fig. S2, A to D). Moreover, while IL-33/TSLP treatment induced both $CD4^+$ T cells and ILC2s to produce type 2 cytokines, Dex only reduced the $CD4^+$ T cell–derived cytokines (Fig. 2, E to I). These findings suggest that ILC2s, but not T_H2 cells, may play a role in the development of steroid-resistant asthma.

ILC2s, but not T_H2 cells, are resistant to steroid-induced apoptosis

Kabata *et al.* (*10*) reported that although cultured ILC2s treated with IL-33 remain steroid sensitive, they become steroid resistant when IL-2 and IL-7 are added. To understand how ILC2s acquire steroid resistance, we used this system as an in vitro model. We isolated ILC2s from the lungs of mice treated intratracheally with IL-33 and differentiated murine T_H2 cells from T cells in splenocytes from naïve mice. Both cell types were then stimulated in vitro with recombinant mouse (rm)IL-2, IL-7, and IL-33 (IL-2/7/33) with and without Dex (Fig. 3A). The cytokine treatment induced both ILC2s and T_H2 cells to proliferate, but Dex did not affect proliferation (fig. S3, A and B). However, Dex induced significant apoptosis in the T_H2 cells, whereas the ILC2s remained unaffected (Fig. 3, B and C). Similarly, Dex reduced the IL-5 and IL-13 production of the T_H2 cells but not the ILC2s (Fig. 3, D to G). Notably, ILC2s required the presence of all three cytokines (IL-2, IL-7, and IL-33) to acquire steroid resistance, as IL-33 alone led to steroid-sensitive ILC2s (fig. S3, C and D). Thus, steroid resistance in ILC2s requires not only IL-33–induced activation but also concurrent IL-33–independent signaling.

We also tested whether IL-2/7/33–stimulated ILC2s from humans exhibited steroid resistance in vitro. When ILC2s isolated from peripheral blood mononuclear cells (PBMCs) of healthy donors were treated with recombinant human (rh)IL-2, IL-7, and IL-33 with or without Dex (Fig. 3H and table S1), the production of type 2 cytokines from ILC2s was not affected by Dex (Fig. 3I). In contrast, T_H2 cells differentiated from naïve $CD4^+$ T cells of healthy PBMCs displayed decreased type 2 cytokine production when treated with Dex (Fig. 3J).

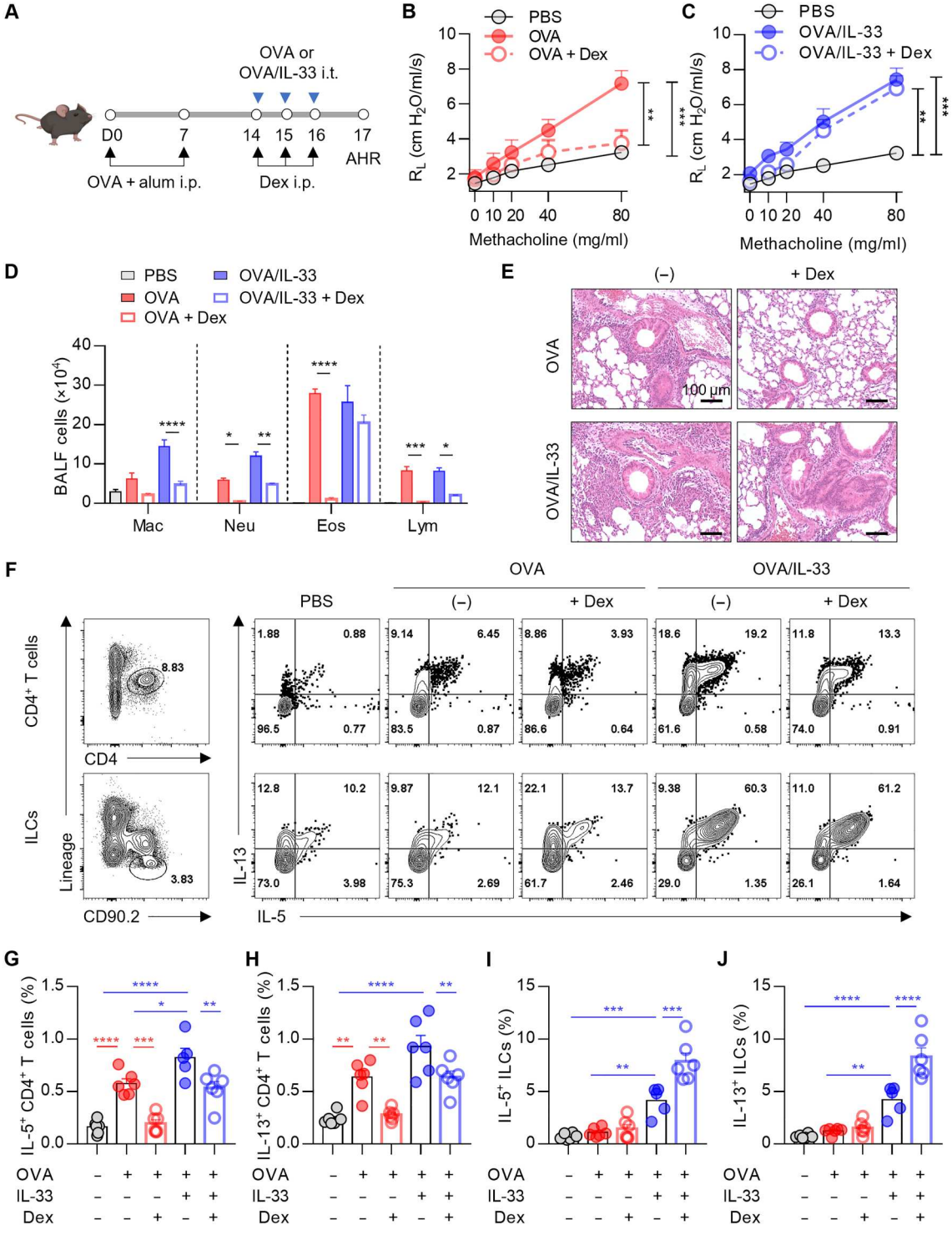

Fig. 1. The steroid resistance in the OVA/IL-33–induced asthma model was associated with the acquisition of steroid resistance by ILC2s but not T_H2 cells. (**A**) Schematic diagram of the asthma models induced by OVA alone and OVA/IL-33. (**B** and **C**) AHR of the OVA-alone (B) and OVA/IL-33 (C) models with or without Dex treatment. (**D** and **E**) Immune-cell numbers in the BALF (D) and H&E staining of the lungs (E) of the OVA-alone and OVA/IL-33 models with or without Dex treatment. Scale bars, 100 μm. (**F** to **J**) Frequencies of IL-5– and IL-13–producing $CD4^+$ T cells (gated as $CD45^+Lineage^+CD4^+$ cells) and ILCs (gated as $CD45^+Lineage^-CD90.2^+$ cells) in the OVA-alone and OVA/IL-33 models with or without Dex treatment. Representative dot plots are shown in (F) and the frequencies of $IL\text{-}5^+$ (G) and $IL\text{-}13^+$ (H) $CD4^+$ T cells and $IL\text{-}5^+$ (I) and $IL\text{-}13^+$ (J) ILC2s are plotted. *$P \leq 0.05$, **$P \leq 0.01$, ***$P \leq 0.001$, and ****$P \leq 0.0001$, by one-way ANOVA followed by Bonferroni's posttest. The data are representative of two to three independent experiments and are presented as mean ± SEM.

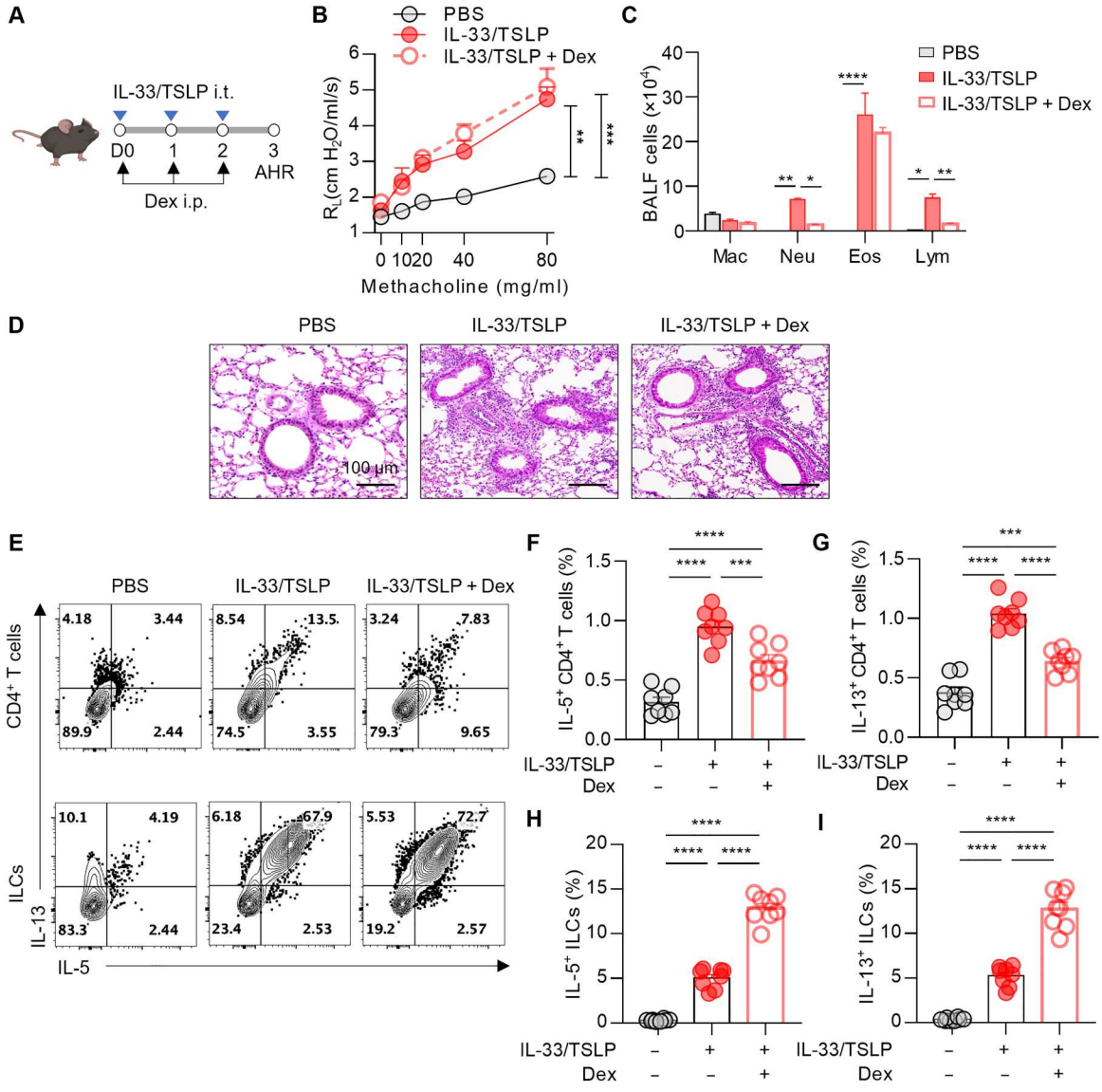

Fig. 2. Activation of ILC2s with TSLP as well as IL-33 induces steroid-resistant asthma. (**A**) Schematic diagram of the IL-33/TSLP-induced asthma model. (**B** to **D**) AHR (B), immune-cell counts in the BALF (C), and H&E staining of the lungs (D) in the IL-33/TSLP model with and without Dex treatment. Scale bars, 100 μm. (**E** to **I**) Frequencies of IL-5– and IL-13–producing $CD4^+$ T cells (gated as $CD45^+Lineage^+CD4^+$ cells) and ILCs (gated as $CD45^+Lineage^-CD90.2^+$ cells) in the IL-33/TSLP model with and without Dex treatment. Representative dot plots are shown in (E). The frequencies of $IL\text{-}5^+$ (F) and $IL\text{-}13^+$ (G) $CD4^+$ T cells and $IL\text{-}5^+$ (H) and $IL\text{-}13^+$ (I) ILC2s are plotted. $^*P \leq 0.05$, $^{**}P \leq 0.01$, $^{***}P \leq 0.001$, and $^{****}P \leq 0.0001$, by one-way ANOVA followed by Bonferroni's posttest. The data are representative of two to three independent experiments and are presented as mean ± SEM.

JAK3 is essential for the survival and type 2 functions of ILC2s

To uncover the signaling pathways responsible for persistent ILC2 activation, we analyzed the RNA sequencing data of a publicly available resource (GSE112937) (*22*), specifically examining nonactivated and activated lung ILC2 RNA datasets. Our analysis revealed that nonactivated and activated ILC2s did not significantly differ in the expression of NF-κB and mitogen-activated protein kinase (MAPK) pathway genes, which are known to operate downstream of IL-33 (*23*). However, activated lung ILC2s exhibited up-regulated expression of the JAK/STAT pathway gene set (Fig. 4A).

In mammals, the JAK family includes four JAKs: JAK1, JAK2, JAK3, and TYK2 (*24*). To determine whether these molecules contribute to the ability of IL-2/7/33 to induce ILC2 activation, we cotreated murine lung ILC2s with various JAK inhibitors, including AZD1480, which suppresses both JAK1 and JAK2 activation (JAK1/2i) and PF06651600, a JAK3 inhibitor (JAK3i). We found that JAK3i, but not JAK1/2i, induced the apoptosis of ILC2s and reduced their proliferation and IL-5 and IL-13 production (Fig. 4, B to E). JAK3i also down-regulated the type 2 cytokine production of ILC2s from human PBMCs (Fig. 4, F and G). We confirmed the importance of JAK3 signaling in ILC2 activation with JANEX-1, which selectively inhibits JAK3 without altering JAK1, JAK2, and

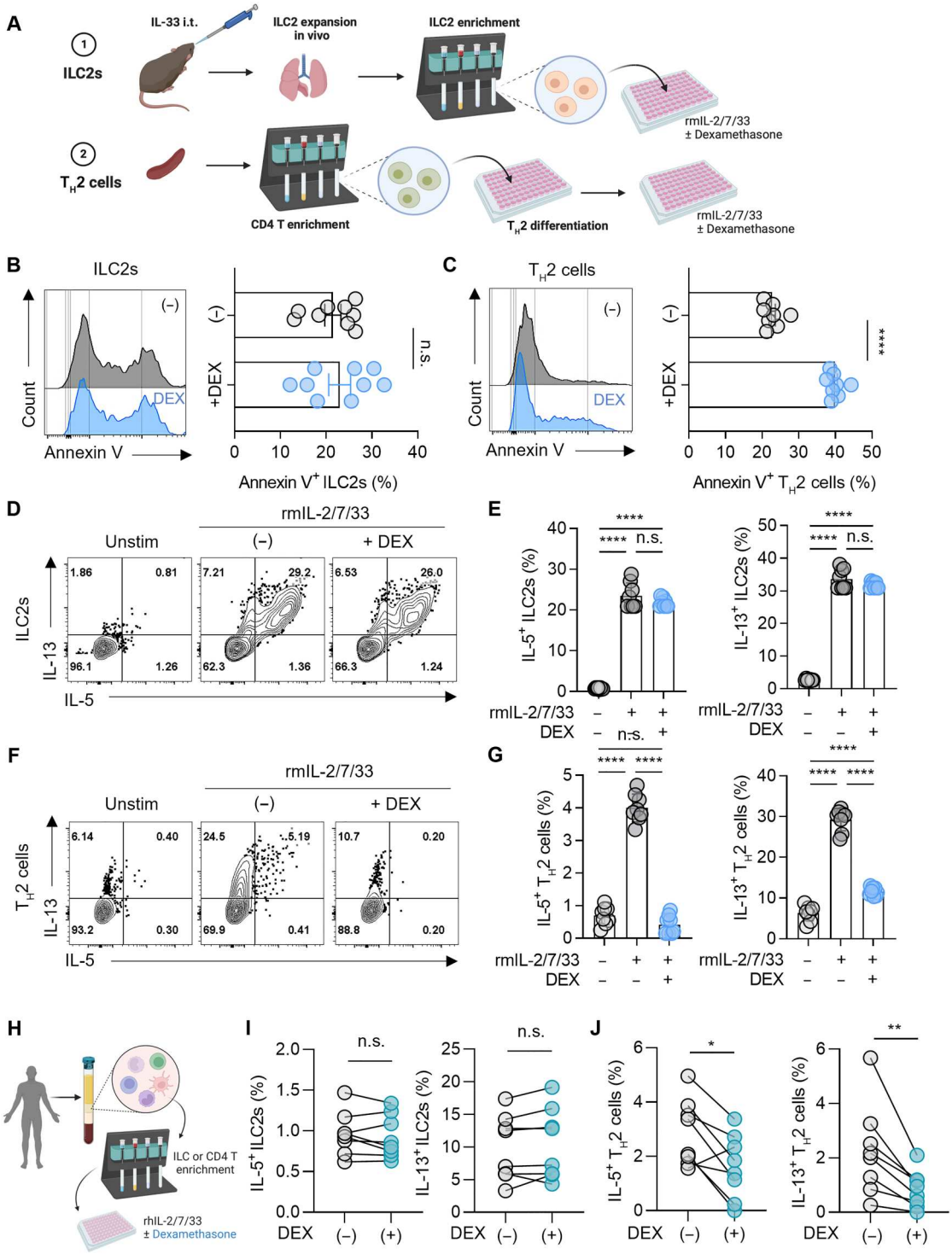

Fig. 3. IL-2/7/33 treatment induces steroid-resistant murine and human ILC2s in vitro but T_H2 cells remain steroid sensitive. (**A**) Schematic diagram showing the isolation of murine lung ILC2s and differentiation of T_H2 cells from naïve murine splenocytes in vitro, and their treatment with IL-2/7/33 with and without Dex. (**B** and **C**) Annexin V expression by the murine ILC2s (B) and T_H2 cells (C). (**D** to **G**) Frequencies of IL-5– and IL-13–producing murine ILC2s [(D) and (E)] and T_H2 cells [(F) and (G)]. Representative dot plots are shown in (D) and (F). The frequencies of IL-5$^+$ and IL-13$^+$ cells are plotted in (E) and (G). (**H**) Schematic diagram of the isolation of ILCs and CD4$^+$ T cells from human PBMCs (n = 10 subjects) and their in vitro treatment with IL-2/7/33 with and without Dex. (**I** to **J**) Frequencies of IL-5$^+$ and IL-13$^+$ ILCs (I) and T_H2 cells (J) are plotted. n.s., not significant; *$P \leq 0.05$, **$P \leq 0.01$, and ****$P \leq 0.0001$, by unpaired t test [(B) and (C)], one-way ANOVA followed by Bonferroni's posttest [(E) and (G)], and paired t test [(I) and (J)]. The data are representative of two to three independent experiments and are presented as mean ± SEM.

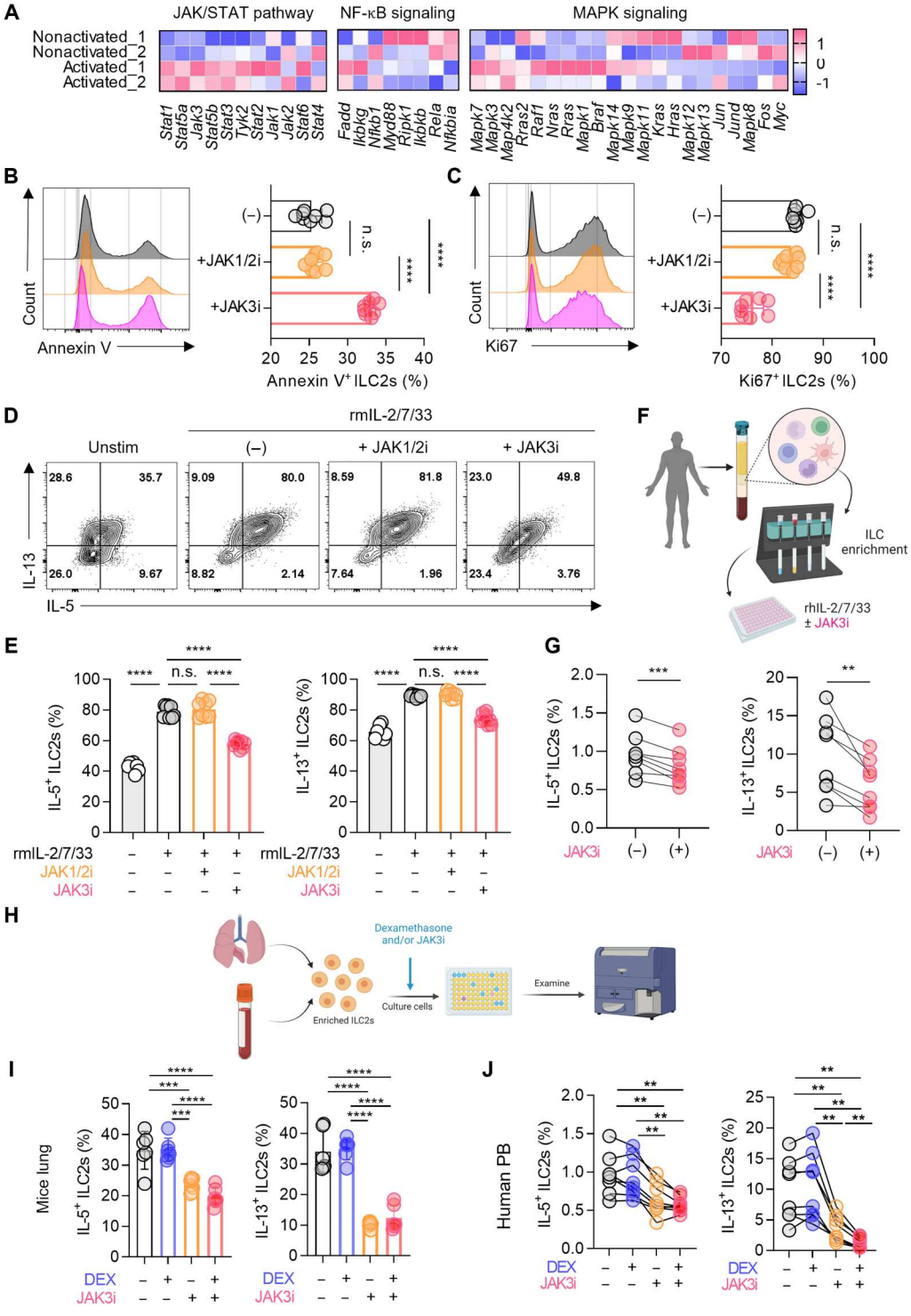

Fig. 4. Murine and human ILC2 activation is regulated by JAK3 and JAK3i inhibits type 2 cytokine production by steroid-resistant ILC2s. (**A**) Identification of the signaling pathways that associate with ILC2 activation by using the publicly available GSE112937 RNA sequences of nonactivated and activated ILC2s. (**B** to **E**) Effect of JAK1/2i or JAK3i treatment on IL-2/7/33–stimulated murine lung ILC2s. Their annexin V (B) and Ki67 (C) expression are shown. Their frequencies of IL-5– and IL-13–producing murine ILC2s are shown by representative dot plots (D) and plots (E). (**F** and **G**) A schematic diagram of human ILC isolation, stimulation with IL-2/7/33, and JAK3i treatment in vitro is shown in (F), and the frequencies of IL-5$^+$ (left) and IL-13$^+$ (right) ILCs (n = 10) are plotted in (G). (**H** to **J**) Effect of Dex and JAK3i treatment on the type 2 cytokine production of murine and human ILC2s. A schematic diagram of the isolation of ILC2s from murine lungs and human PBMCs and their in vitro treatment with Dex and/or JAK3i is shown in (H). The frequencies of IL-5$^+$ and IL-13$^+$ ILC2s in the murine (I) and human (n = 10) (J) samples are shown. n.s., not significant; , $^{**}P \leq 0.01$, $^{***}P \leq 0.001$, and $^{****}P \leq 0.0001$, by one-way ANOVA followed by Bonferroni's posttest [(B), (C), (E), and (I)], paired t test (G), and one-way repeated-measures ANOVA followed by Bonferroni's posttest (J). The data are representative of two to three independent experiments and are presented as mean ± SEM.

other protein tyrosine kinases (*25*). JANEX-1 suppressed the IL-5 and IL-13 production of murine ILC2s (fig. S4, A and B). Although PF06651600 also inhibits Tec protein tyrosine kinase family members, including Bruton's tyrosine kinase (BTK) and interleukin-2-inducible T cell kinase (*26*), Branebrutinib, which inhibits the Tec kinase family (*27*), did not affect ILC2 cytokine production (fig. S4, C and D). Therefore, JAK3 signaling may play a more specific role in activating ILC2s than other signaling pathways.

Next, we investigated whether JAK3i regulates the steroid resistance of ILC2s in vitro (Fig. 4H). Murine lung ILC2s and human ILC2s were stimulated with IL-2/7/33 with and without Dex, and their production of IL-5 and IL-13 was examined. We found that the resistance of the cells to Dex disappeared when JAK3i was

present (Fig. 4, I and J). These results suggest that JAK3 not only appears to be necessary for ILC2 activation, survival, and type 2 functions, but also mediates the steroid resistance of ILC2s. Therefore, JAK3 could be a promising target in therapies that inhibit steroid-resistant ILC2s.

JAK3 signaling induces cytokine multipotency and steroid resistance in ILC2s

JAK mediates the phosphorylation of cytokine receptors′ tyrosine residues, which leads to the recruitment of STAT proteins. The six STAT proteins can then be phosphorylated by JAK on tyrosine residues, causing their dimerization and transport across the nuclear membrane. Once in the nucleus, they can regulate cytokine-responsive gene expression (*28*) (fig. S5A). To determine which STAT contributes to ILC2 steroid resistance, IL-2/7/33–stimulated ILC2s were cultured alone or with different JAK inhibitors, and STAT1 to STAT6 phosphorylation was examined. IL-2/7/33 treatment significantly increased phosphorylation of STAT1, STAT3, STAT5, and STAT6, but not STAT2 or STAT4. All inhibitors blocked STAT1 phosphorylation, while pan-JAKi (Tofacitinib) and JAK3i blocked STAT3, STAT5, and STAT6 phosphorylation (Fig. 5, A and B). Phosphorylation of STAT1 in IL-2/7/33–stimulated ILC2s is regulated by both JAK1/2 and JAK3, while JAK3 alone regulates phosphorylation of STAT3, STAT5, and STAT6. Flow cytometry confirmed that IL-2/7/33 stimulation promoted STAT3 and STAT5 phosphorylation in ILC2s, which was suppressed by JAK3i (fig. S5, B and C). Notably, the STAT3 inhibitor (STAT3i) induced apoptosis in ILC2s, while the STAT6 inhibitor (STAT6i) and STAT5 inhibitor (STAT5i) exhibited only marginal or no impact on apoptosis (Fig. 5C and fig. S5D). However, it is worth noting that when it came to inhibiting proliferation and the production of type 2 cytokines by ILC2s, all three inhibitors were effective, with STAT3i showing the highest efficacy (Fig. 5, C and D, and fig. S5, E and F). Furthermore, we investigated whether JAK3 signaling is STAT specific or involves noncanonical pathways such as MAPK and NF-κB signaling. Our findings revealed that all JAK inhibitors suppressed the phosphorylation of noncanonical pathways without any JAK3i specificity (fig. S5, G and H).

Next, we compared the phosphorylation of STATs in sputum cells from asthma patients and healthy controls (fig. S5, I and J, and table S1). Asthma patient cells contained significantly higher levels of phosphorylated STAT3, STAT5, and STAT6 than healthy donors (fig. S5, I and J). We also observed up-regulation of STAT3, STAT5, and STAT6 phosphorylation in IL-2/7/33–stimulated human ILC2s, which was inhibited by JAK3i (Fig. 5, E to H).

According to reports, the activation of STAT3, STAT5, and STAT6 is mainly associated with type 3, type 1, and type 2 cytokines, respectively (*29*). Here, we observed that the stimulation of IL-2/7/33 up-regulated type 2 cytokine production and induced the phosphorylation of all three of these STATs in ILC2s. To gain a broader understanding of the ILC2 cytokine profile, we examined the effects of IL-2/7/33 treatment in more detail. We found that IL-2/7/33 treatment significantly increased the frequency of ILC2s that coexpressed IL-5, IL-13, and IL-17A (Fig. 5, I and J). Further analysis revealed that the proportion of IL-17A$^+$ ILC2s that coexpressed IL-5 and IL-13 among total ILC2s was increased by IL-2/7/33 (Fig. 5K). We did not observe any expression of interferon-γ (IFN-γ) by ILC2s under any conditions (fig. S6, A and B). These results indicate that IL-2/7/33 treatment can cause ILC2s to produce type 3 as well as type 2 cytokines, which has been observed previously in other settings (*30*, *31*). Further investigation revealed that JAK3i and downstream STAT inhibitors inhibited the multipotent ILC population in vitro, while Dex did not have any significant effect (Fig. 5, L and M, and fig. S6, C and D). However, Dex reduced the production of type 2 cytokines by ILC2s stimulated with IL-33 alone (fig. S3D). Additionally, we observed the presence of multipotent ILC2s coexpressing IL-17A in humans, and these cells were effectively inhibited by JAK3i but not by Dex (fig. S6, E and F). These findings suggest that the acquisition of cytokine multipotency by ILC2s following IL-2/7/33 treatment could potentially mediate the steroid resistance of ILC2s.

JAK3 inhibitor suppresses multipotent ILC2s and ameliorates *Alternaria*-induced asthma

To investigate the potential therapeutic use of JAK3i in ILC2-induced allergic asthma (*8*), we tested the ability of JAK3i to alleviate asthma symptoms using the *Alternaria alternata* (Alt) asthma model. We treated wild-type and *Rag1*$^{-/-}$ mice with Alt extract intratracheally with or without intragastric injection of JAK3i to determine whether the effects of JAK3i were independent of T cells (Fig. 6A and fig. S7A). The intragastric approach was used because JAKi is administered orally in clinical practice (*32*). The results showed that JAK3i significantly reduced AHR and inflammatory cell infiltration in the BALF and lungs of both wild-type and *Rag1*$^{-/-}$ mice (Fig. 6, B to D, and fig. S7, B to D). Histological analysis of lung tissue using hematoxylin and eosin (H&E) staining confirmed that JAK3i ameliorated the infiltration of immune cells around the airways (Fig. 6E and fig. S7E). Further investigation of the cytokines produced by lung ILC2s in the mice revealed that Alt extract treatment increased the production of IL-5 and IL-13 by ILCs, but not T cells (Fig. 6, F and G, and fig. S7, F to I). JAK3i treatment reversed this phenomenon powerfully in both wild-type and *Rag1*$^{-/-}$mice (Fig. 6, F and G, and fig. S7, F and G). Alt extract inoculation alone increased the frequency of multipotent IL-5$^+$IL-13$^+$IL-17A$^+$ ILC2s in the lungs (Fig. 6, H and I, and fig. S7, J and K), which we had previously observed in vitro when treating ILC2s with IL-2/7/33 (Fig. 5, I and J).

To further evaluate the impact of JAK3 inhibition (JAK3i) in the context of a chronic Alt model, we exposed mice to Alt extract over a 3-week period (fig. S8A). Similar to the acute model, JAK3i effectively attenuated AHR and reduced eosinophil infiltration within the airways in the chronic model (fig. S8, B and C). Furthermore, JAK3i had a positive impact on diminishing inflammatory cell infiltration in the lungs, as evidenced by histopathological examination using H&E staining (fig. S8D). It is noteworthy that the chronic Alt model induced the production of type 2 cytokines from both CD4$^+$ T cells and ILCs (fig. S8, E to G). However, while JAK3i did not significantly decrease cytokine production from CD4$^+$ T cells, it exhibited a notable reduction in cytokine production from ILCs (fig. S8, E to G). JAK3i also led to a decrease in the population of multipotent IL-5$^+$IL-13$^+$IL-17A$^+$ ILCs in the context of the chronic Alt model (fig. S8, H and I).

Furthermore, we conducted adoptive transfers of both normal ILC2s and ILC2s treated with JAK3 inhibitor (JAK3i) into *Rag2*$^{-/-}$γc$^{-/-}$ double-knockout mice, which lack ILCs (Fig. 6J). Our findings revealed that the introduction of normal ILC2s led to an increase in AHR and the infiltration of eosinophils in the BALF. Conversely, the transfer of JAK3i-treated ILC2s had no discernible

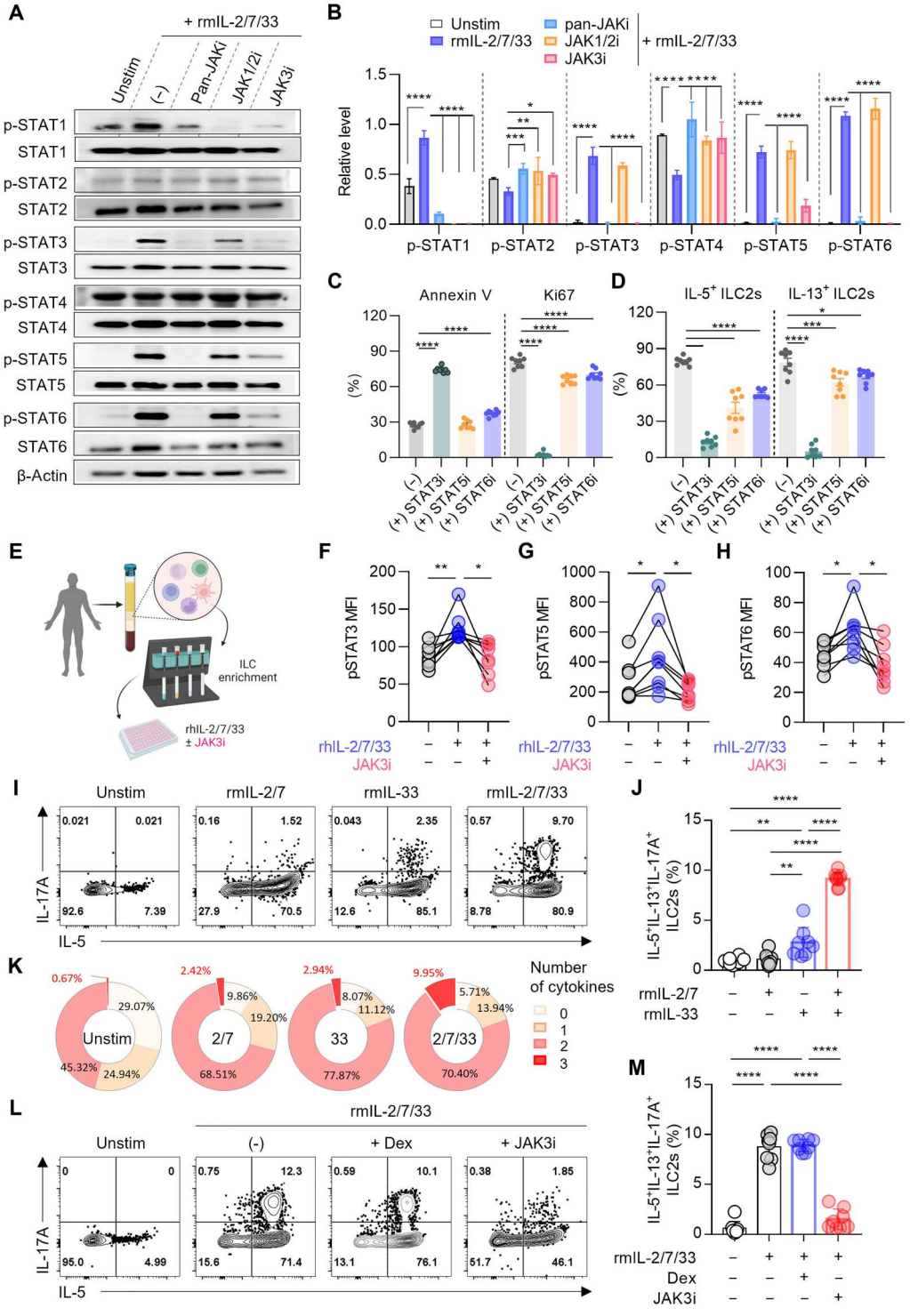

Fig. 5. JAK3 inhibition suppresses STAT3, STAT5, and STAT6 phosphorylation in ILC2s. (**A** and **B**) Western blot analysis of phosphorylated STAT1 to STAT6 in murine ILC2s stimulated with IL-2/3/33 and treated with different JAK inhibitors: Pan-JAKi (Tofacitinib), JAK1/2i (AZD1480), or JAK3i (PF06651600). A representative blot is displayed in (A), and relative phosphorylated STAT levels are depicted in (B). (**C** and **D**) Murine ILC2s, stimulated in vitro with IL-2/7/33, were treated with STAT inhibitors: STAT3i (Stattic), STAT5i (STAT-IN-1), or STAT6i (AS1517499). Frequencies of annexin V$^+$ or Ki67$^+$ ILC2s (C) and IL-5$^+$ or IL-13$^+$ ILC2s (D) are displayed. (**E** to **H**) Human ILCs isolated from PBMCs (n = 10) were stimulated with IL-2/7/33 in vitro and treated with JAK3i. A schematic diagram of the experiment is shown in (E). MFI of the phosphorylated STAT3 (F), STAT5 (G), and STAT6 (H) in the ILC2s in the PBMCs are shown. (**I** to **K**) Murine ILC2s were stimulated with IL-2/7 alone, IL-33 alone, or all three together. The frequencies of IL-5$^+$IL-13$^+$IL-17A$^+$ ILC2s were determined. A representative dot plot is shown in (I) and the cell frequencies were presented in a histogram in (J). The frequencies of ILC2s that expressed none, one, two, or three of the IL-5, IL-13, and IL-17A cytokines are also presented in a pie chart (K). (**L** and **M**) Murine ILC2s were stimulated with IL-2/7/33 with and without Dex or JAK3i. Representative dot plots of the IL-17A–expressing IL-5$^+$ ILC2s are shown in (L). The frequencies of IL-5$^+$IL-13$^+$IL-17A$^+$ ILC2s are plotted in (M). n.s., not significant; *$P \leq 0.05$, **$P \leq 0.01$, ***$P \leq 0.001$, and ****$P \leq 0.0001$, by one-way ANOVA followed by Bonferroni's posttest [(B) to (D), (J), and (M)],, and one-way repeated-measures ANOVA followed by Bonferroni's posttest [(F) to (H)]. The data are representative of two to three independent experiments and are presented as mean ± SEM or ± SD.

effect on these parameters (Fig. 6, K and L). The transferred JAK3i-treated ILC2s produced fewer cytokines than normal ILC2s (Fig. 6, M and N), which strongly confirms the direct effect of JAK3i on ILC2 function in vivo. Together, these findings suggest that the blockade of JAK3 signaling could be a promising therapeutic target for ILC2-induced asthma.

The JAK3 inhibitor shows potent efficacy in treating steroid-resistant asthma

Finally, we investigate the potential of JAK3i as a therapeutic option for steroid-resistant asthma using an OVA/IL-33–induced asthma model. As shown in Fig. 1, asthma in this model is driven by both T cells and ILC2s, but only the T cells are responsive to Dex treatment. To test the efficacy of JAK3i, OVA-injected mice were

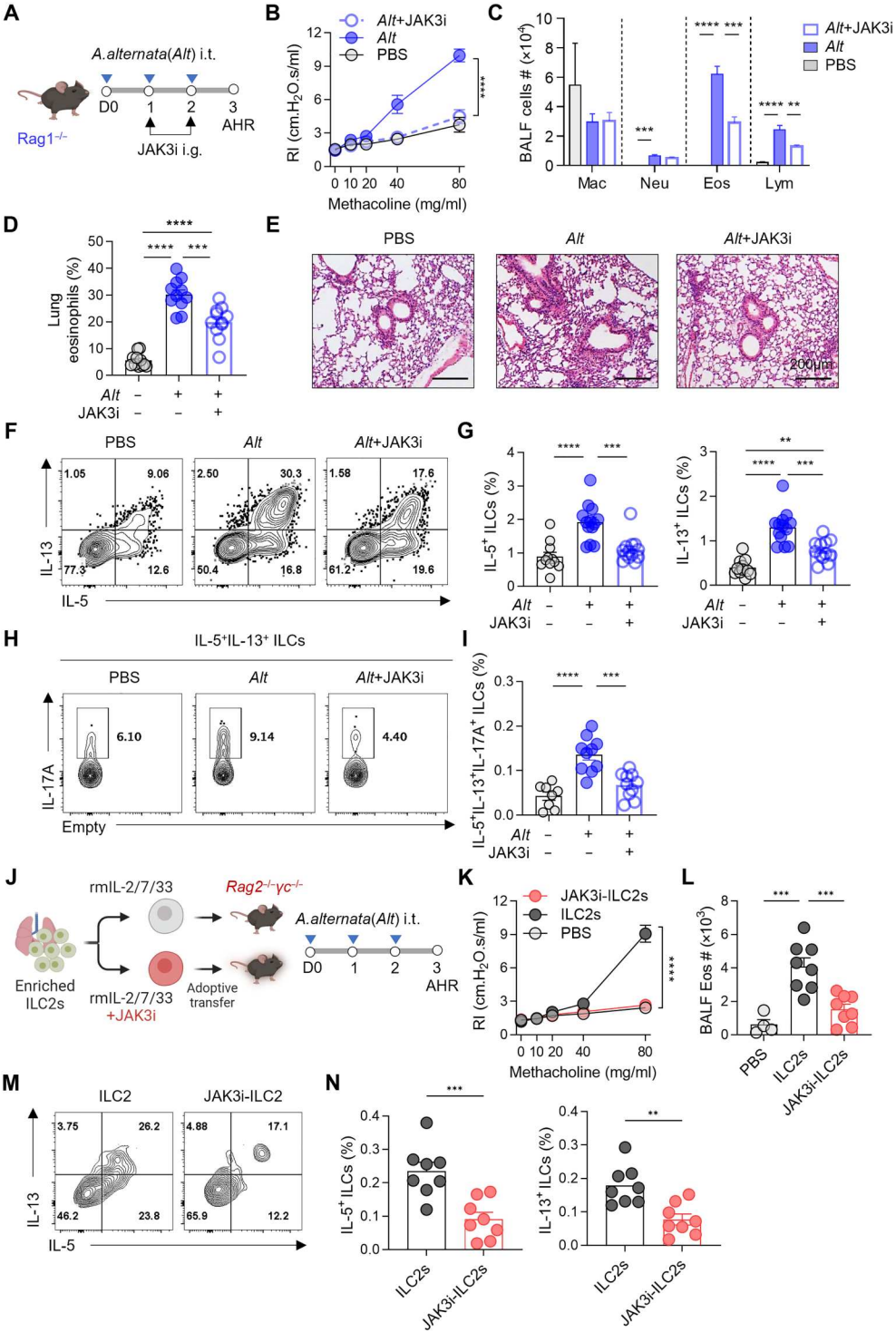

Fig. 6. JAK3 inhibition ameliorates the ILC2-driven moderate asthma in the murine *Alt* extract–induced model. (**A**) Schematic diagram of the *Alt* extract–induced asthma model in *Rag1*$^{-/-}$ mice. (**B**) AHR in the *Rag1*$^{-/-}$ mice. (**C**) Immune-cell counts in the BALF of the *Rag1*$^{-/-}$ mice. (**D**) The frequency of eosinophils (gated as CD45$^+$CD11b$^+$SiglecF$^+$ cells) in lungs. (**E**) H&E staining of the lungs. Scale bars, 200 μm. (**F** and **G**) Frequencies of IL-5– and IL-13–producing ILCs (gated as CD45$^+$Lineage$^-$CD90.2$^+$ cells). Representative dot plots are shown in (F) and the frequencies are plotted in (G). (**H** and **I**) Frequencies of IL-17A–producing IL-5$^+$IL-13$^+$ ILCs (gated as CD45$^+$Lineage$^-$CD90.2$^+$IL-5$^+$IL-13$^+$ cells). Representative dot plots are shown in (H) and the frequencies are plotted in (I). (**J** to **N**) Adoptive transfer of ILC2s treated with or without JAK3i into *Rag2*$^{-/-}$γc$^{-/-}$ mice followed by the induction of the *Alt* extract–induced asthma model. (J) Schematic representation of the experimental model. (K) Evaluation of AHR in *Rag2*$^{-/-}$γc$^{-/-}$ mice that received ILC2 transfers. (L) Enumeration of eosinophils in the BALF of *Rag2*$^{-/-}$γc$^{-/-}$ mice that received ILC2 transfers. (M) Representative dot plots of IL-5 and IL-13 production from transferred ILC2s. (N) The frequencies of the transferred IL-5$^+$ and IL-13$^+$ ILC2s are plotted. $^{**}P \le 0.01$, $^{***}P \le 0.001$, and $^{****}P \le 0.0001$, by unpaired *t* test and one-way ANOVA followed by Bonferroni's posttest. The data are representative of two to three independent experiments and are presented as mean ± SEM.

challenged with OVA/IL-33, with or without Dex and/or JAK3i (Fig. 7A). The results showed that treatment with Dex alone failed to reduce AHR, eosinophil infiltration in BALF, and lung inflammation. Similarly, treatment with JAK3i alone also failed to ameliorate asthma (Fig. 7, B to D). However, when both Dex and JAK3i were administered together, the AHR and inflammatory cell infiltration were potently reduced (Fig. 7, B to D, and fig. S9).

Further analysis revealed that Dex blocked CD4$^+$ T cells but not ILC2 production of type 2 cytokines, while JAK3i had the opposite effect. However, the two treatments together blocked both immune cell types (Fig. 7, E to I). This suggests that CD4$^+$ T cells and ILC2s may produce type 2 cytokines via different signaling pathways. JAK3i reduced the IL-17A–producing lung ILC2 population induced by OVA/IL-33, whereas Dex did not have any effect on

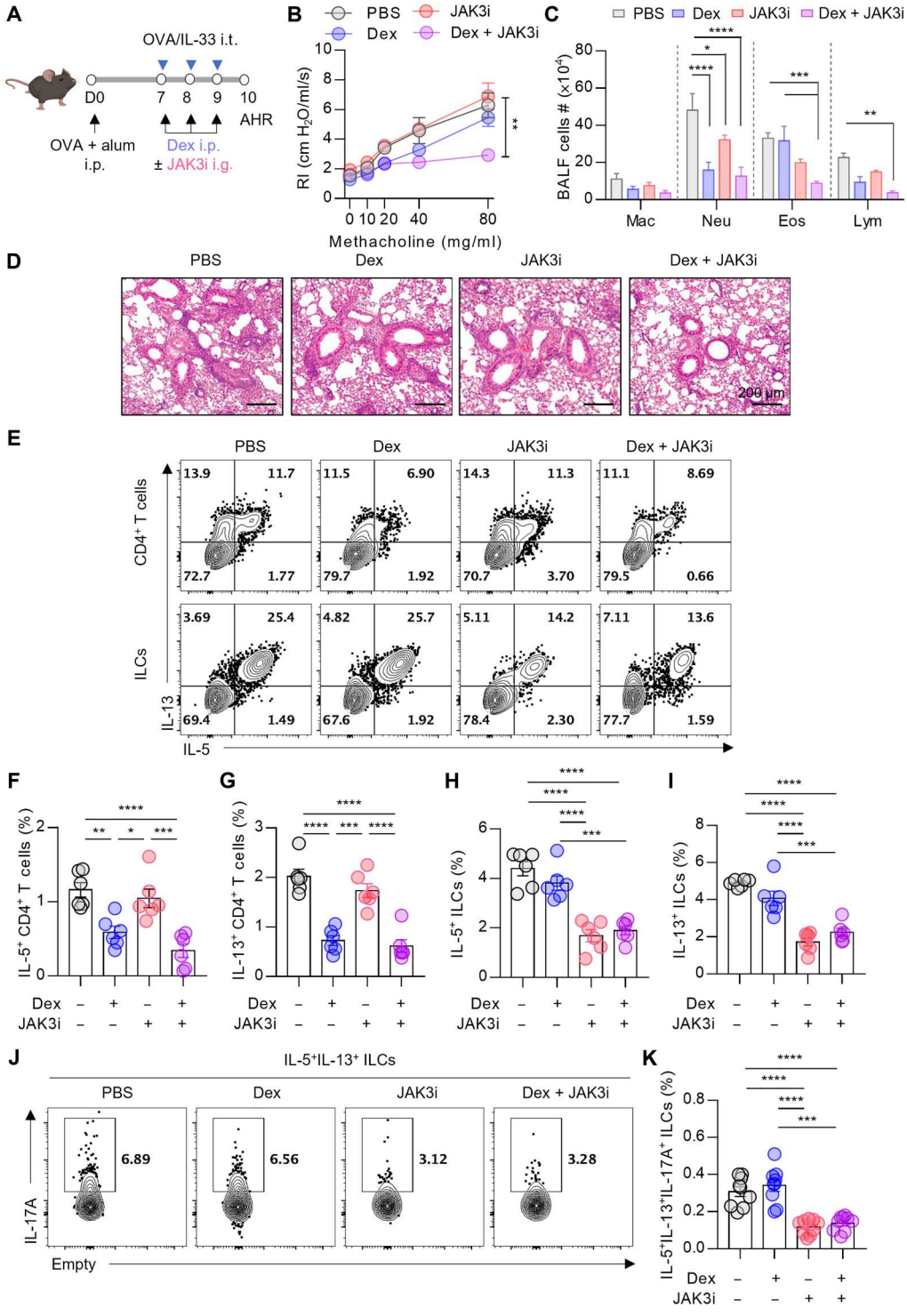

Fig. 7. JAK3 inhibitor ameliorates steroid-resistant asthma when it is administered together with a steroid. (**A**) Schematic diagram of the OVA/IL-33–induced steroid-resistant asthma model and its treatment with Dex and/or JAK3i. (**B**) AHR. (**C**) Immune-cell counts. (**D**) H&E staining of the lungs. Scale bars, 200 μm. (**E** to **I**) Frequencies of IL-5– and IL-13–producing $CD4^+$ T cells (gated as $CD45^+Lineage^+CD4^+$ cells) and ILCs (gated as $CD45^+Lineage^-CD90.2^+$ cells). Representative dot plots are shown in (E). The frequencies of $IL\text{-}5^+$ $CD4^+$ T cells (F), $IL\text{-}13^+$ $CD4^+$ T cells (G), $IL\text{-}5^+$ ILC2s (H), and $IL\text{-}13^+$ ILC2s (I) are plotted. (**J** and **K**) Frequencies of IL-17A–producing $IL\text{-}5^+IL\text{-}13^+$ ILCs (gated as $CD45^+Lineage^-CD90.2^+IL\text{-}5^+IL\text{-}13^+$ cells). Representative dot plots are shown in (J). The frequencies are plotted in (K). $^*P \leq 0.05$, $^{**}P \leq 0.01$, $^{***}P \leq 0.001$, and $^{****}P \leq 0.0001$, by one-way ANOVA followed by Bonferroni's posttest. The data are representative of two to three independent experiments and are presented as mean ± SEM.

this population (Fig. 7, J and K). These findings suggest that JAK3i may improve steroid-resistant asthma by blocking the development of multipotent ILC2s.

Additionally, the effects of Dex and JAK3i on inflammatory cells in the lungs were distinct. Dex treatment reduced the number of neutrophils and DCs, whereas JAK3i did not affect these cell types. Neither treatment alone was able to reduce the number of eosinophils, but the combination of both treatments significantly decreased eosinophilia (fig. S9, A to D). Together, these findings suggest that the combined administration of corticosteroid and JAK3i effectively improved steroid-refractory asthma by inhibiting $CD4^+$ T cells and ILC2s, respectively. Notably, JAK3i may exert its beneficial effect by down-regulating steroid-resistant multipotent lung ILC2s, which could be generated by the combination of ILC-stimulating cytokines that are elicited by asthma triggers.

DISCUSSION

In asthma, corticosteroid resistance is an important clinical issue. Our study used a model of steroid-resistant asthma (OVA/IL-33) driven by both T_H2 cells and ILC2s to show that while the T_H2 cells remain sensitive to Dex, the ILC2s do not. This difference was confirmed in an in vitro model of differential steroid resistance, IL-2/7/33–treated ILC2s, and T_H2 cells. IL-33 itself did not induce ILC2 steroid resistance. Conversely, the combined treatment of IL-2/7/33 induced steroid-resistant ILC2s, and intratracheal inoculation of IL-33 combined with TSLP generated steroid-resistant asthma. Therefore, ILC2s may only acquire steroid resistance when multiple ILC-stimulatory cytokines are present. Analysis of GSE112937 RNA sequencing data then showed that activated ILC2s up-regulated gene sets in the JAK/STAT pathway, but not in the NF-κB and MAPK pathways. In vitro analyses with IL-2/7/33–stimulated ILC2s showed that pharmacological inhibition of JAK3 signaling with JAK3i down-regulated the type 2 cytokine production of these cells. JAK3i was then shown to not only inhibit the type 2 cytokine production of ILC2s in the OVA/IL-33 steroid-resistant asthma model but also strongly ameliorate asthma when administered with Dex. The steroid resistance of both the IL-2/7/33–stimulated in vitro ILC2s and OVA/IL-33–induced asthma was associated with the emergence of a multipotent ($IL\text{-}5^+IL\text{-}13^+IL\text{-}17A^+$) ILC2 population that disappeared when JAK3i was administered. Therefore, ILC2s may acquire steroid resistance via a selective JAK3/STAT pathway stimulated by combinations of cytokines, generating a multipotent ILC2 subpopulation.

There is limited evidence supporting the notion that ILC2s may help mediate steroid-resistant asthma. Nagakumar *et al.* (*9*) found that steroid-resistant asthma patients have more sputum ILC2s than control asthma patients. Smith *et al.* (*33*) also showed that ILC2s, even with strong oral corticosteroid treatment, can cause ongoing airway eosinophilia in severe asthma patients. Meanwhile, Luo *et al.* (*34*) reported that circulating ILC2s from steroid-resistant asthma patients rose after steroid treatment, unlike T_H2 cells. Moreover, van der Ploeg *et al.* (*35*) observed that asthma patients have more inflammatory $CD45RO^+$ ILC2s in the inflamed mucosal tissues and blood of asthma patients than controls. These ILC2 frequencies correlate with disease severity and steroid resistance. They also showed that circulating ILC2s from healthy subjects display steroid resistance. Additionally, Liu *et al.* (*36*) showed that sputum ILC2s from asthma patients were steroid resistant, although circulating ILC2s were not. Furthermore, Kabata *et al.* (*10*) developed the OVA/IL-33 steroid-resistant asthma model in mice that we used in the present study. Like us, they showed that this asthma is associated with the accumulation of steroid-resistant ILC2s in the lungs. These studies thus support the notion that ILC2s could help mediate steroid-refractory asthma.

Several mechanisms by which ILC2s may acquire steroid resistance have been also proposed in previous studies. For instance, Luo *et al.* (*34*) found that peripheral blood ILC2s from healthy subjects express higher levels of the anti-apoptotic genes BCL2 and BCL2L1 and lower levels of the pro-apoptotic genes BAX1 and BAK1 than T_H2 cells. This suggests that ILC2s are less sensitive to the pro-apoptotic effects of steroids than T_H2 cells, which could explain their resistance to steroids. Human studies by Liu *et al.* (*36*) and van der Ploeg *et al.* (*35*) and a mouse study by Kabata *et al.* (*10*) also suggest that TSLP may play an important role in the steroid resistance of ILC2s. Liu *et al.* (*36*) found that the TSLP levels in the sputum of asthma patients correlated with the steroid resistance of the sputum ILC2s. Van der Ploeg *et al.* (*35*) noted that IL-33 and TSLP together convert $CD45RA^+$ ILC2s, which are steroid-sensitive, into steroid-resistant $CD45RO^+$ ILC2s in vitro; TSLP on its own did not have this effect. Kabata *et al.* (*10*) observed that steroid-sensitive murine ILC2s became steroid resistant when stimulated in vitro with both IL-33 and TSLP. Additionally, our study shows that activated ILC2s induced by IL-33 alone are steroid- sensitive and that combining IL-33 with IL-2/7 could generate steroid-resistant ILC2s. Together, these observations suggest that the steroid resistance of ILC2s requires their activation by not only IL-33 but also another stimulant. In the latter case, our in vitro studies confirmed that combining IL-33 with IL-2/7 could generate steroid-resistant ILC2s.

Our study demonstrated that up-regulation of STAT3, STAT5, and STAT6 was associated with ILC2s acquiring steroid resistance. Similarly, Liu *et al.* (*36*) and Kabata *et al.* (*10*) also demonstrated that STAT5 is involved in the induction of steroid resistance in ILC2s. Because STAT3, STAT5, and STAT6 are primarily associated with the production of type 3, type 1, and type 2 cytokines, respectively (*29*), this may explain the emergence of multipotent steroid-resistant ILC2s that produce IL-5, IL-13, and IL-17A in response to IL-2/7/33 treatment in vitro and the lungs of mice with OVA/IL-33–induced asthma. The local inflammatory environment may induce plasticity in ILC2s that enables them to produce both type 3 and type 2 cytokines, which, in turn, may lead to steroid resistance. Previous studies suggest that such multipotent ILC2s can form in specific lung inflammation settings (*30*, *31*). However, the signaling pathway involved in generating these multipotent ILC2s has not been identified. Our findings, which indicate that JAK3 inhibition caused these multipotent ILC2s to disappear, suggest that the JAK/STAT pathway plays a crucial role in this transformation.

The receptors for both IL-2 and IL-7 share the common γ chain (*13*), which activates downstream signaling through the PI3K-Akt, Ras-MAPK, and JAK-STAT pathways (*37*). Our analysis of the GSE112937 RNA sequences revealed that the JAK/STAT pathway likely plays a critical role in ILC2 activation. This finding is supported by the importance of the JAK/STAT pathway in ILC development and maturation (*15*): $Jak3^{-/-}$ mice exhibit reduced numbers of CLP, CHILP, and ILC2P (*38*), while patients with JAK3 and IL-2Rγ mutations lack ILCs (*39*). Additionally, the JAK/STAT pathway also plays substantial roles in ILC2 functions in disease: STAT6

induces the proliferation and amphiregulin secretion of ILC2s in *Alternaria*-induced asthma (*40*), and *Nippostrongylus brasiliensis*–infected STAT6$^{-/-}$ mice exhibit fewer IL-13–producing ILC2s than control-infected mice (*41*). Furthermore, we confirmed that JAK3 inhibition induced apoptosis, decreased proliferation, and reduced type 2 cytokine expression in ILC2s stimulated in vitro with IL-2/7/33. This not only supports the notion that the JAK/STAT pathway plays a critical role in ILC2 activation but also suggests that inhibiting this pathway may be a potential therapeutic strategy for managing steroid-resistant asthma.

Our study revealed that while both T_H2 and ILC2 cells contribute to asthma in the OVA/IL-33 model, only the T_H2 cells were sensitive to steroids, while the ILC2s were not. In contrast, the ILC2s became sensitive to JAK3i, whereas the T_H2 cells did not. Despite expressing the same cytokine receptors and glucocorticoid receptors (GRs) (*12*, *42*–*44*), the reasons for these differences in JAK3i and steroid sensitivity are unclear. However, the differential sensitivity to JAK3i may relate to varying levels of IL-7 receptor (IL-7R) expression. While high IL-7R levels are required for the survival and proliferation of naive and memory T cells, T cell receptor signaling downregulates IL-7R expression in activated effector T cells (*45*, *46*). It means that T_H2 cells are not dependent on the downstream signaling pathways of IL-7R for their survival and functions, which explains why JAK3i did not affect them. Conversely, activated ILC2s maintain high IL-7R expression, which is critical for their survival, proliferation, and function (*47*), making them sensitive to JAK3i. Likewise, the different sensitivities of T_H2 cells and ILC2s to steroids may be related to differences in the expression patterns of GR isoforms. The gene encoding GR produces two isoforms by alternative splicing, GR-α and GR-β (*48*). GR-α, the major GR isoform, binds steroids with high affinity (*49*), whereas GR-β does not and instead inhibits GR-α (*50*, *51*). It is possible that upon exposure to OVA/IL-33 or IL-2/7/33, ILC2s upregulate their GR-β expression, leading to steroid resistance, while T_H2 cells do not, resulting in steroid sensitivity. This notion is supported by several studies showing that GR-β expression in multiple BALF and PBMC cells is associated with steroid insensitivity in asthma (*52*, *53*). Future studies on the GR isoforms expressed by T_H2 cells and ILC2s in steroid-resistant asthma are warranted.

JAK inhibitors have emerged as a promising class of drugs for treating various immune-mediated disorders. Ruxolitinib, a JAK1/JAK2 inhibitor, is used to treat myeloproliferative neoplasms (*54*), while Tofacitinib is approved for patients with methotrexate-resistant rheumatoid arthritis and psoriatic arthritis (*55*, *56*). Additionally, Baricitinib, a JAK1 and JAK2 inhibitor, has been approved by European regulatory agencies for rheumatoid arthritis (*57*), and Oclacitinib, a pan-JAK inhibitor, has been approved for allergic dermatitis in dogs (*58*). Although JAK inhibitors are not yet approved for asthma, preclinical studies have shown their potential as a treatment option for this disease. Several JAK inhibitors, including P6 (a pan-JAK inhibitor), R256 (a JAK1/3 inhibitor), and Tofacitinib, have been shown to reduce eosinophil numbers, eotaxin, and IL-13 levels in the BALF of mice with OVA-induced asthma (*59*–*61*). Moreover, inhaled JAK inhibitor iJAK-001 has been shown to suppress BALF eosinophilia in mice challenged with *Alternaria* extract in a dose-dependent manner (*62*). In addition, Tofacitinib administered orally has been found to effectively suppress BALF neutrophilia in the lung caused by inhaled LPS (*63*). Therefore, the currently available JAK inhibitors may have the potential to be repurposed for treating steroid-resistant asthma.

In conclusion, our study suggests that in specific circumstances that trigger asthma, a localized inflammatory environment can lead to the emergence of steroid-resistant multipotent ILC2s that contribute to steroid-refractory asthma. Our findings also indicate that JAK3 inhibitors can effectively alleviate steroid-resistant allergic asthma by reducing these multipotent ILC2s in conjunction with steroids. This discovery implies that JAK3 inhibitors may offer a promising therapeutic strategy to overcome corticosteroid resistance in asthma. Additionally, the sensitivity of ILC2s to JAK3 inhibitors suggests that these inhibitors could have therapeutic applications in various ILC2-related diseases (*64*).

MATERIALS AND METHODS

Mice

C57BL/6 mice (ages 6 to 8 weeks) were purchased from Koatech (Gyeonggi-do, South Korea). *Rag1*$^{-/-}$ mice on the C57BL/6 background were purchased from the Jackson Laboratory (ME, USA). *Rag2*$^{-/-}$γc$^{-/-}$ mice were purchased from the Taconic Biosciences (NY, USA). All animals were housed in a specific pathogen–free animal facility at Seoul National University Hospital (Seoul, South Korea).

Mouse models of asthma

To induce the asthma model in Figs. 1 and 7, mice were injected intraperitoneally with 100 μg of OVA (Sigma-Aldrich, MO, USA) and 2 mg of alum adjuvant (Thermo Fisher Scientific, CA, USA). A week later, 50 μg of OVA with or without 250 ng of recombinant mouse IL-33 (BioLegend, CA, USA) was inoculated via intratracheal injection on the indicated days (Figs. 1A and 7A). The asthma model used in Fig. 2 was generated by intratracheal inoculation of 250 ng of IL-33 and 100 ng of TSLP (R&D Systems, MN, USA). To test the steroid resistance of all models, the mice were treated with 5 mg/kg Dex (Sigma-Aldrich, MO, USA) via intraperitoneal injection. The asthma models used in Fig. 6 and figs. S7 and S8 were generated by intratracheal inoculation of 10 μg of *A. alternata* extract (Greer, NC, USA). In Fig. 6, we adoptively transferred 3 × 10^5 ILC2s treated with rmIL-2/7/33 alone or in combination with a JAK3 inhibitor (JAK3i) into *Rag2*$^{-/-}$γc$^{-/-}$ mice. Subsequently, we induced an asthma model in these mice by injecting *Alternaria* extract (Fig. 6J). In some experiments, the mouse models in Figs. 6 and 7 and fig. S8 were inoculated with JAK3-selective inhibitor (10 mg/kg, PF06651600; Sigma-Aldrich) via intragastric injection.

Measurement of AHR

AHR was measured by an invasive measurement system Buxco FinePointe Resistance and Compliance (DSI, MN, USA). Mice were anesthetized with an intraperitoneal injection of pentobarbital sodium (150 mg/kg), tracheotomized, and intubated with an 18-gauge stainless steel catheter. Airflow and lung resistance were monitored after the methacholine (Sigma-Aldrich, MO, USA) challenge in a dose-dependent manner.

Histological analysis

To measure immune cell infiltration into the lungs, whole lung tissue was fixed with 4% paraformaldehyde and embedded in paraffin for sectioning. The paraffin blocks were cut into 4-μm-thick

sections, and H&E staining was performed to analyze the pathological changes and airway inflammation.

Differential counting of immune cells in BALF

To measure immune cell infiltration into BALF, BALF cells were attached to slide glass by using cytospin and then stained with Diff Quik solution (Sysmex Corporation, Japan) according to the manufacturer′s instructions. Macrophages, neutrophils, eosinophils, and lymphocytes were identified based on their morphology and counted.

Preparation of cells from murine lungs

To isolate single cells from lungs, lung tissues were digested with RPMI 1640 media (Welgene, Gyeongsangbuk-do, South Korea) supplemented with collagenase type IV (1 mg/ml; Worthington Biochemical Corp, NJ, USA) and DNase I (0.5 mg/ml; Sigma-Aldrich, MO, USA) for 90 min at 37°C. The digested tissues were filtered with 40-μm cell strainer and the red blood cells (RBCs) were lysed with RBC lysis buffer (BioLegend, CA, USA). To isolate the ILC2s from the lungs, mice were treated intratracheally with 500 ng of IL-33 (BioLegend) for 3 consecutive days and, after 7 days, the lungs were digested as described above. The ILC2s were then isolated with the EasySep Mouse Pan-ILC Enrichment Kit (STEMCELL Technologies Inc., Vancouver, Canada).

T_H2 cell differentiation

To induce T_H2 cell differentiation, the spleen from naïve mice was ground in a 40-μm strainer and the RBCs were lysed with RBC lysis buffer (BioLegend, CA, USA). The splenocytes were then cultured with CellXVivo Mouse T_H2 Cell Differentiation Kit (R&D Systems, MN, USA) according to the manufacturer′s instructions.

Human subjects and sample preparation

We recruited 10 healthy donors and four asthma patients from the Department of Internal Medicine, Seoul National University Hospital (Seoul, South Korea). The asthma patients all met the following criteria: they had chronic respiratory symptoms (e.g., coughing, mucus hyperproduction, dyspnea, and wheezing) and were positive on the bronchial provocation test that was used to confirm AHR [defined as <16 mg/ml methacholine induced a 20% fall of forced expiratory volume in 1 s (FEV_1)]. Blood samples were obtained from the healthy donors and centrifuged at 2000 rpm for 10 min at 4°C to separate the blood cells from the plasma. To isolate the PBMCs, the blood cells were diluted with phosphate-buffered saline (PBS), loaded on Ficoll-Paque PLUS density gradient medium (GE Healthcare, IL, USA), and centrifuged at 1800 rpm for 25 min at room temperature without braking. The PBMC layer was collected from the buffy coat and washed with PBS. The isolated PBMCs were then stored with Cellbanker I (Zenoaq, Japan) at −80°C. Human ILC2s were isolated from PBMCs with the EasySep Human Pan-ILC Enrichment Kit (STEMCELL Technologies Inc., Vancouver, Canada). Human naïve $CD4^+$ T cells were isolated with the Mojosort Human CD4 Naive T cell Isolation Kit (BioLegend, CA, USA) and differentiated to T_H2 cells using CellXVivo Human T_H2 Cell Differentiation Kit (R&D systems, MN, USA). Induced sputum was obtained from the healthy donors and asthma patients and incubated with 0.1% dithiothreitol (Sigma-Aldrich, MO, USA) for 20 min at 37°C to eliminate the mucus. It was then filtered with a 70 μm strainer and centrifuged to obtain the pellet. The pellet was lysed with radioimmunoprecipitation assay (RIPA) lysis buffer (Biosesang, Gyeonggi-do, South Korea) for Western blotting analysis.

In vitro treatment of murine and human cells with Dex and inhibitors

Murine ILC2s and T_H2 cells cultured in RPMI 1640 (Welgene, Gyeongsangbuk-do, South Korea) supplemented with 10% fetal bovine serum (Biowest, MO, USA) and gentamicin (10 μg/ml; Biowest) were activated with recombinant mouse (rm)IL-2, IL-7, and IL-33 (20 ng/ml; all from BioLegend, CA, USA) for 3 days at 37°C. Human ILC2s and T_H2 cells were cultured in the same medium and activated with recombinant human (rh)IL-2, IL-7, and IL-33 (20 ng/ml; all from BioLegend) for 3 days at 37°C. In some experiments, the cells were treated for the same duration with 100 nM Dex (Sigma-Aldrich, MO, USA), 10 nM pan-JAK inhibitor (Tofacitinib; Sigma-Aldrich), 5 nM JAK1/2 inhibitor (AZD1480; Sigma-Aldrich), 50 nM JAK3 inhibitor (PF06651600; Sigma-Aldrich), 78 μM JANEX-1 (MedChemExpress, NJ, USA), 1 nM Branebrutinib (MedChemExpress), 10 μM STAT3 inhibitor (Stattic; R&D systems, MN, USA), 50 μM STAT5 inhibitor (STAT-IN-1; MedChemExpress), and/or 30 nM STAT6 inhibitor (AS1517499; MedChemExpress).

Flow cytometry

Single cells that were isolated from tissues were stained with the Zombie Aqua Fixable Viability Kit (BioLegend, CA, USA) to exclude dead cells, blocked with anti-CD16/CD32 (BD Bioscience, NJ, USA), and surface stained with the following fluorochrome-labeled monoclonal antibodies for 30 min at 4°C: anti-CD3ε (clone 145-2C11, BD Bioscience), anti-CD4 (RM4–5, BioLegend), anti-CD11b (M1/70, BD Bioscience), anti-CD11c (HL3, BD Bioscience), anti-CD19 (ID3, BD Bioscience), anti-CD45 (30-F11, BioLegend), anti-CD49b (DX5, BD Bioscience), anti-CD90.2 (30-H12, BioLegend), anti-F4/80 (BM8, BioLegend), anti-FcεRIα (MAR-1, BioLegend), anti-$I\text{-}A^b$ (AF6–120.1, BioLegend), anti-Ly6G (1A8, BioLegend), and anti-SiglecF (E50–2440, BD Bioscience). For intracellular cytokine staining, the cells were stimulated with phorbol 12-myristate 13-acetate (PMA, 100 ng/ml; Sigma-Aldrich, MO, USA) and ionomycin (1 μg/ml; Sigma-Aldrich) in the presence of GolgiStop (BD Bioscience) in RPMI 1640 (Welgene, Gyeongsangbuk-do, South Korea) supplemented with 10% fetal bovine serum (Biowest, MO, USA) and gentamicin (10 μg/ml; Biowest) for 3 hours at 37°C. After surface staining, the cells were fixed and permeabilized with the Cytofix/Cytoperm kit (BD Bioscience) and stained with anti–IL-5 (TRFK5, BioLegend), anti–IL-13 (eBio13A, Invitrogen, CA, USA), anti–IFN-γ (XMG1.2, BioLegend), and anti–IL-17A (TC11-18H10.1, BioLegend) antibodies. To identify apoptotic cells, surface-stained cells were stained with an annexin V staining kit (BioLegend). To identify proliferating cells, surface-stained cells were fixed and permeabilized with the Foxp3/Transcription Factor Staining Buffer Set (Invitrogen) and then stained with anti-Ki67 (16A8, BioLegend). To measure the phosphorylated form of proteins intracellularly, surface-stained cells were fixed with fixation buffer (BioLegend), permeabilized with True-Phos Perm Buffer (BioLegend), and then stained with anti-pSTAT3 (Tyr705; 13A3–1, BioLegend), anti-pSTAT5 (Tyr694; 47/Stat5, BD Bioscience), and anti-pSTAT6 (Tyr641; CHI2S4N, Invitrogen) antibodies. To stain human cells, cultured ILC2s and T_H2

cells were stimulated with PMA and ionomycin, as indicated above. Surface molecules were stained with anti-CD45 (clone HI30, BioLegend), anti-CD3ε (UCHT1, BioLegend), anti-CD4 (A161A1, BioLegend), anti-CD11c (3.9, BioLegend), anti-CD11b (ICRF44, BioLegend), anti-CD14 (HCD14, BioLegend), anti-CD19 (HIB19, BioLegend), anti-CD49b (P1E6-C5, BioLegend), anti-CD127 (A019D5, BioLegend), and anti-FcεRIα (AER-37, BioLegend). The cells were then fixed and permeabilized with the Cytofix/Cytoperm kit (BD Bioscience) and stained with anti-IL-5 (JES1-39D10, BioLegend) and anti-IL-13 (JES10-5A2, BioLegend) antibodies. Flow cytometry was performed using BD LSRFortessa X-20 and BD LSR II and the data were analyzed by FlowJo (V10.2) software.

Western blot

ILC2s that were stimulated with cytokines and inhibitors or the sputum pellet of human subjects were lysed with RIPA lysis buffer (Biosesang, Gyeonggi-do, South Korea) and centrifuged at 13,000 rpm for 10 min at 4°C. The protein concentration was quantified with a Bradford assay. The same amount of protein per sample was loaded onto 8% tris-glycine SDS-polyacrylamide gels and electroblotted on polyvinylidene difluoride membranes. The membranes were blocked at room temperature for 1 hour with 5% bovine serum albumin (BSA; Bovogen biologicals, VIC, Australia) in tris-buffered saline with 0.1% Tween 20 (0.1% TBS-T) to analyze the phosphorylated form of proteins or in 5% skim milk in 0.1% TBS-T to analyze the total protein form. The blocked membranes were incubated with the following primary antibodies overnight at 4°C: phospho-STAT1 (clone D4A7, Cell Signaling Technology, MA, USA), phospho-STAT2 (polyclonal, Bioss, MA, USA), phospho-STAT3 (D3A7, Cell Signaling Technology), phospho-STAT4 (polyclonal, Bioss), phospho-STAT5 (D47E7, Cell Signaling Technology), phospho-STAT6 (D8S9Y, Cell Signaling Technology), Stat Antibody Sampler Kit II (Cell Signaling Technology), phospho-MEK1/2 (41G9, Cell Signaling Technology), phospho-ERK1/2 (polyclonal, Cell Signaling Technology), phospho-p38 (D3F9, Cell Signaling Technology), phospho-JNK (G9, Cell Signaling Technology), phospho-p65 (93H1, Cell Signaling Technology), MEK1/2 (D1A5, Cell Signaling Technology), ERK1/2 (polyclonal, Cell Signaling Technology), p38 (D13E1, Cell Signaling Technology), JNK (polyclonal, Cell Signaling Technology), IκBα (L35A5, Cell Signaling Technology), and β-actin (polyclonal, Bioss). The cells were then incubated at room temperature for 1 hour with the appropriate horseradish peroxidase–conjugated secondary antibodies in 0.1% TBS-T.

Study approval

All animal experiments were approved by the Institutional Animal Care and Use Committee in Seoul National University Hospital (SNUH-IACUC 19–0106) and all animals were maintained according to the *Guide for the Care and Use of Laboratory Animals Eighth Edition*, NRC (2010) in a facility accredited by Association for Assessment and Accreditation of Laboratory Animal Care (AAALAC) International (#001169). All human subjects who were enrolled in this study provided written informed consent. The study protocol was approved by the Seoul National University Hospital Institutional Review Board (IRB numbers 1607-148-778 and 1810-036-977).

Statistics

To analyze the normality of the data, the Shapiro-Wilk normality test was conducted. Two groups were compared by using the Mann-Whitney test or unpaired *t* test. To compare multiple groups, a one-way analysis of variance (ANOVA) followed by Bonferroni's posttest was conducted. To analyze the treatment-induced changes per sample relative to baseline, a paired *t* test or one-way repeated-measures ANOVA followed by Bonferroni's posttest was used. The data were expressed as mean ± SEM or SD. *P* values less than 0.05 were considered significant. All statistics were performed with GraphPad Prism 7.

Supplementary Materials

This PDF file includes:

Figs. S1 to S9

Table S1

REFERENCES AND NOTES

1. S. T. Holgate, S. Wenzel, D. S. Postma, S. T. Weiss, H. Renz, P. D. Sly, Asthma. *Nat. Rev. Dis. Primers* **1**, 15025 (2015).
2. J. V. Fahy, Type 2 inflammation in asthma—Present in most, absent in many. *Nat. Rev. Immunol.* **15**, 57–65 (2015).
3. B. N. Lambrecht, H. Hammad, The immunology of asthma. *Nat. Immunol.* **16**, 45–56 (2015).
4. R. Beasley, J. Harper, G. Bird, I. Maijers, M. Weatherall, I. D. Pavord, Inhaled corticosteroid therapy in adult asthma. Time for a new therapeutic dose terminology. *Am. J. Respir. Crit. Care Med.* **199**, 1471–1477 (2019).
5. P. J. Barnes, Efficacy of inhaled corticosteroids in asthma. *J. Allergy Clin. Immunol.* **102**, 531–538 (1998).
6. A. J. Woolcock, Steroid resistant asthma: What is the clinical definition? *Eur. Respir. J.* **6**, 743–747 (1993).
7. C. Nunes, A. M. Pereira, M. Morais-Almeida, Asthma costs and social impact. *Asthma Res. Pract.* **3**, 1 (2017).
8. S. Helfrich, B. C. Mindt, J. H. Fritz, C. U. Duerr, Group 2 innate lymphoid cells in respiratory allergic inflammation. *Front. Immunol.* **10**, (2019).
9. P. Nagakumar, F. Puttur, L. G. Gregory, L. Denney, L. Fleming, A. Bush, C. M. Lloyd, S. Saglani, Pulmonary type-2 innate lymphoid cells in paediatric severe asthma: Phenotype and response to steroids. *Eur. Respir. J.* **54**, 1801809 (2019).
10. H. Kabata, K. Moro, K. Fukunaga, Y. Suzuki, J. Miyata, K. Masaki, T. Betsuyaku, S. Koyasu, K. Asano, Thymic stromal lymphopoietin induces corticosteroid resistance in natural helper cells during airway inflammation. *Nat. Commun.* **4**, 2675 (2013).
11. H. H. Walford, S. J. Lund, R. E. Baum, A. A. White, C. M. Bergeron, J. Husseman, K. J. Bethel, D. R. Scott, N. Khorram, M. Miller, D. H. Broide, T. A. Doherty, Increased ILC2s in the eosinophilic nasal polyp endotype are associated with corticosteroid responsiveness. *Clin. Immunol.* **155**, 126–135 (2014).
12. Q. N. Yu, Y. B. Guo, X. Li, C. L. Li, W. P. Tan, X. L. Fan, Z. L. Qin, D. Chen, W. P. Wen, S. G. Zheng, Q. L. Fu, ILC2 frequency and activity are inhibited by glucocorticoid treatment via STAT pathway in patients with asthma. *Allergy* **73**, 1860–1870 (2018).
13. Y. Rochman, R. Spolski, W. J. Leonard, New insights into the regulation of T cells by γc family cytokines. *Nat. Rev. Immunol.* **9**, 480–490 (2009).
14. C. J. Dwyer, H. M. Knochelmann, A. S. Smith, M. M. Wyatt, G. O. Rangel Rivera, D. C. Arhontoulis, E. Bartee, Z. Li, M. P. Rubinstein, C. M. Paulos, Fueling cancer immunotherapy with common gamma chain cytokines. *Front. Immunol.* **10**, 263 (2019).
15. H. Stabile, G. Scarno, C. Fionda, A. Gismondi, A. Santoni, M. Gadina, G. Sciumè, JAK/STAT signaling in regulation of innate lymphoid cells: The gods before the guardians. *Immunol. Rev.* **286**, 148–159 (2018).
16. G. Sciumè, M. T. Le, M. Gadina, HiJAKing innate lymphoid cells? *Front. Immunol.* **8**, 438 (2017).
17. M. V. Aun, R. Bonamichi-Santos, F. M. Arantes-Costa, J. Kalil, P. Giavina-Bianchi, Animal models of asthma: Utility and limitations. *J. Asthma Allergy* **10**, 293–301 (2017).
18. H. H. Raissy, H. W. Kelly, M. Harkins, S. J. Szefler, Inhaled corticosteroids in lung diseases. *Am. J. Respir. Crit. Care Med.* **187**, 798–803 (2013).
19. J. Kim, S. Ryu, H. Y. Kim, Innate lymphoid cells in tissue homeostasis and disease pathogenesis. *Mol. Cells* **44**, 301–309 (2021).

20. G. M. Gauvreau, R. Sehmi, C. S. Ambrose, J. M. Griffiths, Thymic stromal lymphopoietin: Its role and potential as a therapeutic target in asthma. *Expert Opin. Ther. Targets* **24**, 777–792 (2020).
21. G. Eberl, M. Colonna, J. P. D. Santo, A. N. J. McKenzie, Innate lymphoid cells: A new paradigm in immunology. *Science* **348**, aaa6566 (2015).
22. T. Y. F. Halim, B. M. J. Rana, J. A. Walker, B. Kerscher, M. D. Knolle, H. E. Jolin, E. M. Serrao, L. Haim-Vilmovsky, S. A. Teichmann, H. R. Rodewald, M. Botto, T. J. Vyse, P. G. Fallon, Z. Li, D. R. Withers, A. N. J. McKenzie, Tissue-restricted adaptive type 2 immunity is orchestrated by expression of the costimulatory molecule OX40L on group 2 innate lymphoid cells. *Immunity* **48**, 1195–1207.e6 (2018).
23. S. M. Pinto, Y. Subbannayya, D. A. B. Rex, R. Raju, O. Chatterjee, J. Advani, A. Radhakrishnan, T. S. Keshava Prasad, M. R. Wani, A. Pandey, A network map of IL-33 signaling pathway. *J. Cell. Commun. Signal* **12**, 615–624 (2018).
24. G. R. Stark, I. M. Kerr, B. R. Williams, R. H. Silverman, R. D. Schreiber, How cells respond to interferons. *Annu. Rev. Biochem.* **67**, 227–264 (1998).
25. E. A. Sudbeck, X. P. Liu, R. K. Narla, S. Mahajan, S. Ghosh, C. Mao, F. M. Uckun, Structure-based design of specific inhibitors of Janus kinase 3 as apoptosis-inducing antileukemic agents. *Clin. Cancer Res.* **5**, 1569–1582 (1999).
26. H. Xu, M. I. Jesson, U. I. Seneviratne, T. H. Lin, M. N. Sharif, L. Xue, C. Nguyen, R. A. Everley, J. I. Trujillo, D. S. Johnson, G. R. Point, A. Thorarensen, I. Kilty, J.-B. Telliez, PF-06651600, a dual JAK3/TEC family kinase inhibitor. *ACS Chem. Biol.* **14**, 1235–1242 (2019).
27. S. H. Watterson, Q. Liu, M. B. Bertrand, D. G. Batt, L. Li, M. A. Pattoli, S. Skala, L. Cheng, M. T. Obermeier, R. Moore, Z. Yang, R. Vickery, P. A. Elzinga, L. Discenza, C. D'Arienzo, K. M. Gillooly, T. L. Taylor, C. Pulicicchio, Y. Zhang, E. Heimrich, K. W. McIntyre, Q. Ruan, R. A. Westhouse, I. M. Catlett, N. Zheng, C. Chaudhry, J. Dai, M. A. Galella, A. J. Tebben, M. Pokross, J. Li, R. Zhao, D. Smith, R. Rampulla, A. Allentoff, M. A. Wallace, A. Mathur, L. Salter-Cid, J. E. Macor, P. H. Carter, A. Fura, J. R. Burke, J. A. Tino, Discovery of branebrutinib (BMS-986195): A strategy for identifying a highly potent and selective covalent inhibitor providing rapid in vivo inactivation of Bruton's tyrosine kinase (BTK). *J. Med. Chem.* **62**, 3228–3250 (2019).
28. S. Aittomäki, M. Pesu, Therapeutic targeting of the Jak/STAT pathway. *Basic Clin. Pharmacol. Toxicol.* **114**, 18–23 (2014).
29. X. Hu, J. Li, M. Fu, X. Zhao, W. Wang, The JAK/STAT signaling pathway: From bench to *clinic*. *Signal Transduct. Target Ther.* **6**, 402 (2021).
30. Y. Huang, L. Guo, J. Qiu, X. Chen, J. Hu-Li, U. Siebenlist, P. R. Williamson, J. F. Urban Jr., W. E. Paul, IL-25-responsive, lineage-negative KLRG1(hi) cells are multipotential 'inflammatory' type 2 innate lymphoid cells. *Nat. Immunol.* **16**, 161–169 (2015).
31. T. Cai, J. Qiu, Y. Ji, W. Li, Z. Ding, C. Suo, J. Chang, J. Wang, R. He, Y. Qian, X. Guo, L. Zhou, H. Sheng, L. Shen, J. Qiu, IL-17-producing ST2(+) group 2 innate lymphoid cells play a pathogenic role in lung inflammation. *J. Allergy Clin. Immunol.* **143**, 229–244.e9 (2019).
32. S. N. Georas, P. Donohue, M. Connolly, M. E. Wechsler, JAK inhibitors for asthma. *J. Allergy Clin. Immunol.* **148**, 953–963 (2021).
33. S. G. Smith, R. Chen, M. Kjarsgaard, C. Huang, J. P. Oliveria, P. M. O'Byrne, G. M. Gauvreau, L. P. Boulet, C. Lemiere, J. Martin, P. Nair, R. Sehmi, Increased numbers of activated group 2 innate lymphoid cells in the airways of patients with severe asthma and persistent airway eosinophilia. *J. Allergy Clin. Immunol.* **137**, 75–86.e8 (2016).
34. J. Luo, Y. Wu, R. Shrimanker, S. Go, Y. Ye, C. Hardman, J. Nahler, Y.-L. Chen, L. Stöger, N. Zeng, W. Liu, L. Reed, A. M. Tolkovsky, P. Klenerman, G. Ogg, I. D. Pavord, L. Xue, Resistance to apoptosis underpins the corticosteroid insensitivity of group 2 innate lymphoid cells. *J. Allergy Clin. Immunol.* **144**, 1722–1726.e10 (2019).
35. E. K. van der Ploeg, K. Golebski, M. van Nimwegen, J. R. Fergusson, B. A. Heesters, I. Martinez-Gonzalez, C. M. A. Kradolfer, S. van Tol, B. P. Scicluna, M. J. W. de Bruijn, G. M. de Boer, G. A. Tramper-Stranders, G.-J. Braunstahl, W. F. J. van IJcken, A. P. Nagtegaal, C. M. van Drunen, W. J. Fokkens, D. Huylebroeck, H. Spits, R. W. Hendriks, R. Stadhouders, S. M. Bal, Steroid-resistant human inflammatory ILC2s are marked by CD45RO and elevated in type 2 respiratory diseases. *Sci. Immunol.* **6**, eabd3489 (2021).
36. S. Liu, M. Verma, L. Michalec, W. Liu, A. Sripada, D. Rollins, J. Good, Y. Ito, H. Chu, M. M. Gorska, R. J. Martin, R. Alam, Steroid resistance of airway type 2 innate lymphoid cells from patients with severe asthma: The role of thymic stromal lymphopoietin. *J. Allergy Clin. Immunol.* **141**, 257–268.e6 (2018).
37. J. X. Lin, W. J. Leonard, The common cytokine receptor γ chain family of cytokines. *Cold Spring Harb. Perspect. Biol.* **10**, (2018).
38. M. L. Robinette, M. Cella, J. B. Telliez, T. K. Ulland, A. D. Barrow, K. Capuder, S. Gilfillan, L. L. Lin, L. D. Notarangelo, M. Colonna, Jak3 deficiency blocks innate lymphoid cell development. *Mucosal Immunol.* **11**, 50–60 (2018).
39. F. Vély, V. Barlogis, B. Vallentin, B. Neven, C. Piperoglou, M. Ebbo, T. Perchet, M. Petit, N. Yessaad, F. Touzot, J. Bruneau, N. Mahlaoui, N. Zucchini, C. Farnarier, G. Michel, D. Moshous, S. Blanche, A. Dujardin, H. Spits, J. H. W. Distler, A. Ramming, C. Picard, R. Golub, A. Fischer, E. Vivier, Evidence of innate lymphoid cell redundancy in humans. *Nat. Immunol.* **17**, 1291–1299 (2016).
40. T. A. Doherty, N. Khorram, J. E. Chang, H.-K. Kim, P. Rosenthal, M. Croft, D. H. Broide, STAT6 regulates natural helper cell proliferation during lung inflammation initiated by Alternaria. *Am. J. Physiol. Lung Cell. Mol. Physiol.* **303**, L577–L588 (2012).
41. H. E. Liang, R. L. Reinhardt, J. K. Bando, B. M. Sullivan, I. C. Ho, R. M. Locksley, Divergent expression patterns of IL-4 and IL-13 define unique functions in allergic immunity. *Nat. Immunol.* **13**, 58–66 (2011).
42. J. Zhu, T helper 2 (Th2) cell differentiation, type 2 innate lymphoid cell (ILC2) development and regulation of interleukin-4 (IL-4) and IL-13 production. *Cytokine* **75**, 14–24 (2015).
43. R. K. Gurram, J. Zhu, Orchestration between ILC2s and Th2 cells in shaping type 2 immune responses. *Cell. Mol. Immunol.* **16**, 225–235 (2019).
44. A. H. Miller, R. L. Spencer, B. D. Pearce, T. L. Pisell, Y. Azrieli, P. Tanapat, H. Moday, R. Rhee, B. S. McEwen, Glucocorticoid receptors are differentially expressed in the cells and tissues of the immune system. *Cell. Immunol.* **186**, 45–54 (1998).
45. K. S. Schluns, W. C. Kieper, S. C. Jameson, L. Lefrançois, Interleukin-7 mediates the homeostasis of naïve and memory CD8 T cells in vivo. *Nat. Immunol.* **1**, 426–432 (2000).
46. R. Mazzucchelli, S. K. Durum, Interleukin-7 receptor expression: Intelligent design. *Nat. Rev. Immunol.* **7**, 144–154 (2007).
47. A. Sheikh, N. Abraham, Interleukin-7 receptor alpha in innate lymphoid cells: More than a marker. *Front. Immunol.* **10**, (2019).
48. I. J. Encío, S. D. Detera-Wadleigh, The genomic structure of the human glucocorticoid receptor. *J. Biol. Chem.* **266**, 7182–7188 (1991).
49. S. M. Hollenberg, C. Weinberger, E. S. Ong, G. Cerelli, A. Oro, R. Lebo, E. B. Thompson, M. G. Rosenfeld, R. M. Evans, Primary structure and expression of a functional human glucocorticoid receptor cDNA. *Nature* **318**, 635–641 (1985).
50. K. Hecht, J. Carlstedt-Duke, P. Stierna, J. Gustafsson, M. Brönnegård, A. C. Wikström, Evidence that the beta-isoform of the human glucocorticoid receptor does not act as a physiologically significant repressor. *J. Biol. Chem.* **272**, 26659–26664 (1997).
51. C. M. Bamberger, A. M. Bamberger, M. de Castro, G. P. Chrousos, Glucocorticoid receptor beta, a potential endogenous inhibitor of glucocorticoid action in humans. *J. Clin. Invest.* **95**, 2435–2441 (1995).
52. D. Y. M. Leung, Q. Hamid, A. Vottero, S. J. Szefler, W. Surs, E. Minshall, G. P. Chrousos, D. J. Klemm, Association of glucocorticoid insensitivity with increased expression of glucocorticoid receptor β. *J. Exp. Med.* **186**, 1567–1574 (1997).
53. Q. A. Hamid, S. E. Wenzel, P. J. Hauk, A. Tsicopoulos, B. Wallaert, J. J. Lafitte, G. P. Chrousos, S. J. Szefler, D. Y. Leung, Increased glucocorticoid receptor β in airway cells of glucocorticoid-insensitive asthma. *Am. J. Respir. Crit. Care Med.* **159**, 1600–1604 (1999).
54. B. Li, R. K. Rampal, Z. Xiao, Targeted therapies for myeloproliferative neoplasms. *Biomark. Res* **7**, 15 (2019).
55. D. van der Heijde, Y. Tanaka, R. Fleischmann, E. Keystone, J. Kremer, C. Zerbini, M. H. Cardiel, S. Cohen, P. Nash, Y. W. Song, D. Tegzová, B. T. Wyman, D. Gruben, B. Benda, G. Wallenstein, S. Krishnaswami, S. H. Zwillich, J. D. Bradley, C. A. Connell; ORAL Scan Investigators, Tofacitinib (CP-690,550) in patients with rheumatoid arthritis receiving methotrexate: Twelve-month data from a twenty-four-month phase III randomized radiographic study. *Arthritis Rheum.* **65**, 559–570 (2013).
56. D. Gladman, W. Rigby, V. F. Azevedo, F. Behrens, R. Blanco, A. Kaszuba, E. Kudlacz, C. Wang, S. Menon, T. Hendrikx, K. S. Kanik, Tofacitinib for psoriatic arthritis in patients with an inadequate response to TNF inhibitors. *N. Engl. J. Med.* **377**, 1525–1536 (2017).
57. I. Urits, J. Israel, H. Hakobyan, G. Yusin, G. Lassiter, N. Fackler, A. A. Berger, H. Kassem, A. Kaye, O. Viswanath, Baricitinib for the treatment of rheumatoid arthritis. *Reumatologia* **58**, 407–415 (2020).
58. S. B. Cosgrove, J. A. Wren, D. M. Cleaver, D. D. Martin, K. F. Walsh, J. A. Harfst, S. L. Follis, V. L. King, J. F. Boucher, M. R. Stegemann, Efficacy and safety of oclacitinib for the control of pruritus and associated skin lesions in dogs with canine allergic dermatitis. *Vet. Dermatol.* **24**, 479–e114 (2013).
59. Y. Matsunaga, H. Inoue, S. Fukuyama, H. Yoshida, A. Moriwaki, T. Matsumoto, K. Matsumoto, Y. Asai, M. Kubo, A. Yoshimura, Y. Nakanishi, Effects of a Janus kinase inhibitor, pyridone 6, on airway responses in a murine model of asthma. *Biochem. Biophys. Res. Commun.* **404**, 261–267 (2011).
60. E. Kudlacz, M. Conklyn, C. Andresen, C. Whitney-Pickett, P. Changelian, The JAK-3 inhibitor CP-690550 is a potent anti-inflammatory agent in a murine model of pulmonary eosinophilia. *Eur. J. Pharmacol.* **582**, 154–161 (2008).
61. S. Ashino, K. Takeda, H. Li, V. Taylor, A. Joetham, P. R. Pine, E. W. Gelfand, Janus kinase 1/3 signaling pathways are key initiators of TH2 differentiation and lung allergic responses. *J. Allergy Clin. Immunol.* **133**, 1162–1174.e4 (2014).
62. M. Caniga, H. Yu, H. H. Lee, M. Wang, D. Witter, M. Salmon, P. W. Fan, Estimation of fraction dissolved after intratracheal delivery of a potent Janus kinase inhibitor, iJAK-001, with low solubility in rat and sheep: Impact of preclinical PKPD on inhaled human dose projection. *J. Aerosol Med. Pulm. Drug Deliv.* **32**, 251–265 (2019).

63. E. Calama, I. Ramis, A. Domènech, C. Carreño, J. De Alba, N. Prats, M. Miralpeix, Tofacitinib ameliorates inflammation in a rat model of airway neutrophilia induced by inhaled LPS. *Pulm. Pharmacol. Ther.* **43**, 60–67 (2017).
64. T. Y. Halim, Group 2 innate lymphoid cells in disease. *Int. Immunol.* **28**, 13–22 (2016).

Acknowledgments: We thank the staff at the Seoul National University animal facility as well as the FACS facility staff for expert support and assistance. Additionally, we extend our thanks to the members of the Mucosal Immunology laboratory for constructive criticism and suggestions, **Funding:** This research was supported by the National Research Foundation of Korea (2022R1A2C3007730, 2021R1C1C201005113, SRC2017R1A5A1014560, and RS-2023-0021779). **Author contributions:** Conceptualization: J.K. and H.Y.K. Methodology: J.K. and H.Y.K. Investigation: J.K. and J.H. Visualization: J.K. Funding acquisition: J.K. and H.Y.K. Project administration: J.K., H.R.K., Y.-S.B., T.K., and H.Y.K. Supervision: T.K. and H.Y.K. Writing—original draft: J.K. and H.Y.K. Writing—review and editing: J.K. and H.Y.K. **Competing interests:** The authors declare that they have no competing interests. **Data and materials availability:** All data needed to evaluate the conclusions in the paper are present in the paper and/or the Supplementary Materials. The dataset analyzed in this study is available in the NCBI Gene Expression Omnibus (GSE112937).

Submitted 21 April 2023
Accepted 17 November 2023
Published 20 December 2023
10.1126/sciadv.adi3770